

AD-A113 945

DEFENSE COMMUNICATIONS ENGINEERING CENTER RESTON VA  
PERFORMANCE ANALYSIS OF DIGITAL LOS LINK, MANILA EMBASSY - SANT--ETC(U)  
DEC 81 N J BOROVACU, D SMITH, D E PARKER

F/8 17/2.1  
SANT--ETC(U)

UNCLASSIFIED

DCEC-TR-26-81

ML

For  
S. 100

10

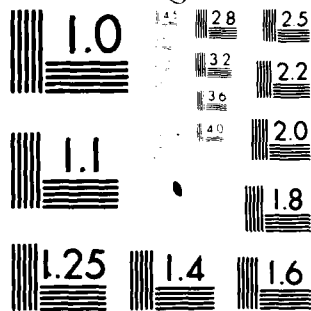
END

DATE

FILED

5-82

DTIC



MICROCOPY RESOLUTION TEST CHART  
NATIONAL BUREAU OF STANDARDS-1963-A

8

TR 26-81



DEFENSE COMMUNICATIONS ENGINEERING CENTER

AD A11 3045

TECHNICAL REPORT NO. 26-81

PERFORMANCE ANALYSIS OF DIGITAL  
LOS LINK, MANILA EMBASSY-  
SANTA RITA, PHILIPPINES

DECEMBER 1981



APPROVED FOR PUBLIC RELEASE; DISTRIBUTION UNLIMITED

8 2 0 4 0 6 1 1 0

DTIC FILE COPY

UNCLASSIFIED R230 26 January 1982  
TY CLASSIFICATION OF THIS PAGE (When Data Entered)

REPORT DOCUMENTATION PAGE		READ INSTRUCTIONS BEFORE COMPLETING FORM
1. REPORT NUMBER DCEC TR 26-81	2. GOVT ACCESSION NO. 110-4113045	3. RECIPIENT'S CATALOG NUMBER
4. TITLE (and Subtitle)  PERFORMANCE ANALYSIS OF DIGITAL LOS LINK MANILA EMBASSY - SANTA RITA, PHILIPPINES		5. TYPE OF REPORT & PERIOD COVERED  Technical Report
		6. PERFORMING ORG. REPORT NUMBER
7. AUTHOR(s) N. J. Sorovacu D. Smith D. E. Parker		8. CONTRACT OR GRANT NUMBER(s)
9. PERFORMING ORGANIZATION NAME AND ADDRESS Defense Communications Engineering Center Transmission Engineering Directive R200 1860 Wiehle Avenue, Reston, VA 22090		10. PROGRAM ELEMENT, PROJECT, TASK AREA & WORK UNIT NUMBERS  N/A
11. CONTROLLING OFFICE NAME AND ADDRESS  (Same as 9)		12. REPORT DATE December 1981
		13. NUMBER OF PAGES 81
14. MONITORING AGENCY NAME & ADDRESS (if different from Controlling Office)  N/A		15. SECURITY CLASS. (of this report)  Unclassified
		15a. DECLASSIFICATION/DOWNGRADING SCHEDULE N/A
16. DISTRIBUTION STATEMENT (of this Report)  A. Approved for public release; distribution unlimited.		
17. DISTRIBUTION STATEMENT (of the abstract entered in Block 20, if different from Report)  N/A		
18. SUPPLEMENTARY NOTES  Review relevance 5 years from submission date.		
19. KEY WORDS (Continue on reverse side if necessary and identify by block number) Link Performance                      Ducting Path Profile                              Diversity Mode Digital Upgrade                          Antenna Radiation Pattern LOS Path Fading		
20. ABSTRACT (Continue on reverse side if necessary and identify by block number)  The U.S. Navy has been tasked to upgrade DCS microwave link M1433, Santa Rita - U.S. Embassy, Philippines, to digital operation using the DRAMA equipment. Impact on bit error rate performance of the new digital radio link caused by a reflection path on Manila Bay is being evaluated in this analysis. Recommendations are made for a link configuration expected to provide an optimum performance in concert with DCS criteria.		

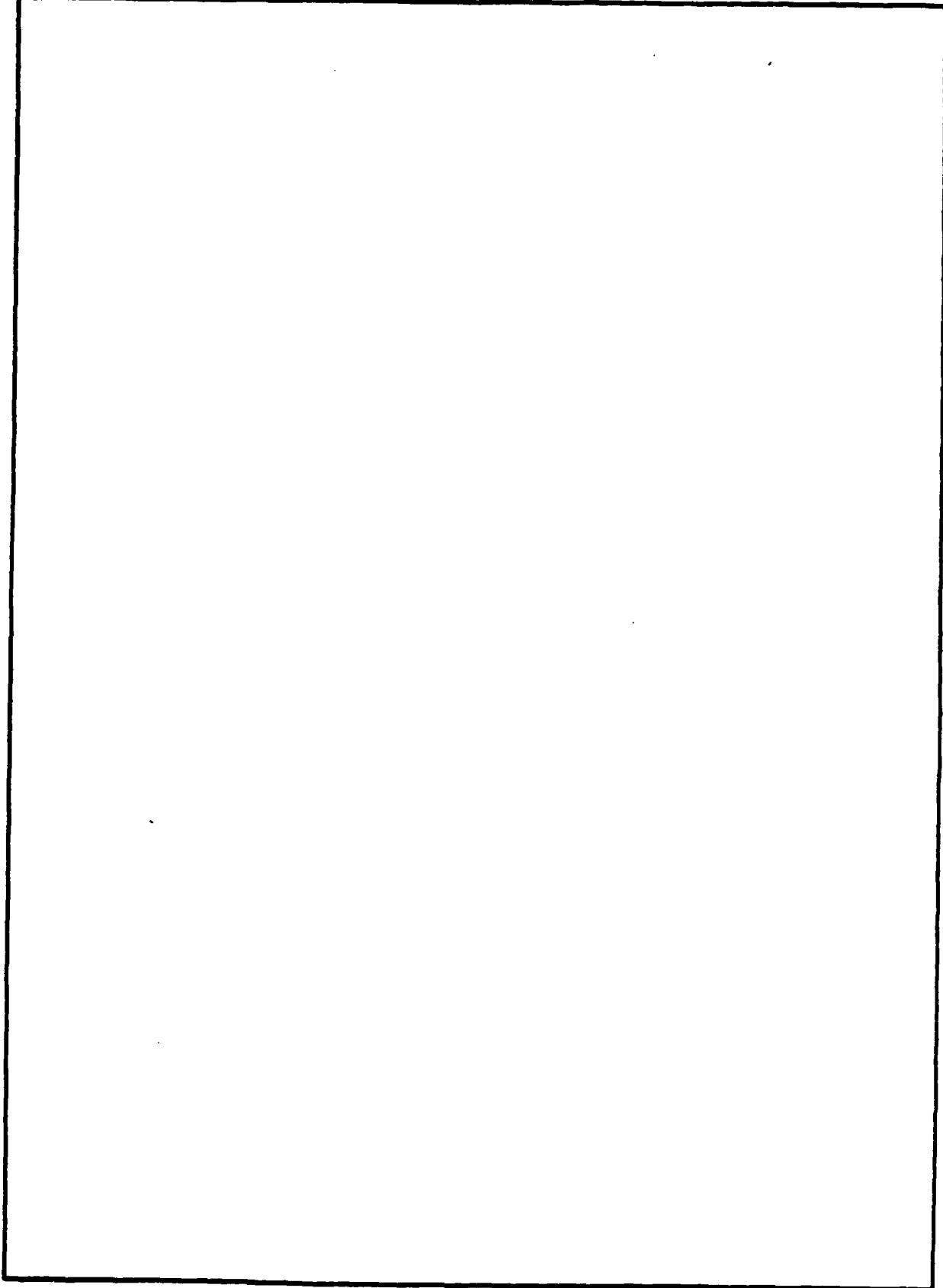
DD FORM 1 JAN 73 1473

EDITION OF 1 NOV 65 IS OBSOLETE

UNCLASSIFIED

SECURITY CLASSIFICATION OF THIS PAGE (When Data Entered)

SECURITY CLASSIFICATION OF THIS PAGE(When Data Entered)



SECURITY CLASSIFICATION OF THIS PAGE(When Data Entered)

TECHNICAL REPORT NO. 26-81


PERFORMANCE ANALYSIS OF DIGITAL LOS LINK,  
MANILA EMBASSY - SANTA RITA, PHILIPPINES

DECEMBER 1981


Prepared by:

- N. Sorovacu
- D. Smith
- D. E. Parker

Technical Content Approved:

  
DANIEL M. JONES  
Colonel, USA  
Deputy Director for  
Transmission Engineering

Approved for Release:

  
R. E. LYONS  
Principal Deputy Director

FOREWORD

The Defense Communications Engineering Center Technical Reports (TR's) are published to inform interested members of the defense community regarding technical activities of the Center, completed and in progress. They are intended to stimulate thinking, encourage information exchange, and provide guidance for related planning and research. They are not an integral part of the DoD PPBS cycle and should not be interpreted as a source of program guidance.

Comments or technical inquiries concerning this document are welcome, and should be directed to:

Director  
Defense Communications Engineering Center  
1860 Wiehle Avenue  
Reston, Virginia 22090



Accession For	
NTIS GRA&I	<input checked="" type="checkbox"/>
DTIC TAB	
Unannounced	
Justification	
By	
Distribution	
Availability	
Dist	
A	

## EXECUTIVE SUMMARY

This Technical Report (TR) contains the performance analysis and recommendations for an optimum implementation of the DCS microwave link between Santa Rita and the U.S. Embassy in the Republic of the Philippines scheduled for a digital upgrade in FY 82 and FY 83. The content of this TR is structured as follows:

a. The purpose of this analysis is introduced in section I, followed-up with a summary of the actions leading to such an analysis in the "Background" section II.

b. In Section III, the performance expected to be derived from the subject link is assessed in terms of the path clearance for various K-factor values ranging from 0.34 to 1.67 and associated Fresnel zones varying from values of 0.3 to 11.0. The degradation in link performance caused by various types of fading is defined in terms of power loss in the receive signal level (RSL), and appropriate corrective actions. The link performance is derived for alternatives in link configuration obtained through various diversity modes, antenna sizes, transmitter power levels, and receiver noise figures.

c. An optimum link configuration is recommended in Section IV. It consists of DCS standard equipment utilizing 12 feet parabolic antennas arranged in a dual space diversity configuration and the DRAMA radio equipment. A minimum of 120 feet height would be required at the U.S. Embassy location for an adequate path clearance to the existing antenna tower heights at Santa Rita. The DRAMA radio equipment is specified for maximum transmit power and a minimum noise figure.

d. The conclusions are presented in Section V. Additional supporting technical material and a synopsis of on-going DoD test and evaluation activities for characterization of service fading effects on digital LOS paths are included in Appendixes A to D.

## TABLE OF CONTENTS

	<u>Page</u>
EXECUTIVE SUMMARY	iii
I. INTRODUCTION	1
II. BACKGROUND	2
III. LINK PERFORMANCE ANALYSIS	4
1. Areas of Concern	4
2. Yearly K Factor Distribution	4
3. Path Profiles	5
4. Performance Degradation Caused by Normal Fading	5
a. Multipath Flat Fading	10
b. Multipath Frequency Selective Fading	10
5. Performance Degradation Caused by Abnormal Fading	15
a. Sub- and Superrefractive Fading	15
b. Ducting	19
c. Rain Attenuation	19
6. Summary of Expected Performance Degradation	24
7. Expected Link Performance	24
IV. RECOMMENDED LINK CONFIGURATION	29
V. CONCLUSIONS	31
REFERENCES	32
APPENDIXES	
A Determining the K Factor to Use in LOS Microwave Links	A-1
B Fading Characteristics for Over-the-Water Microwave Links	B-1
C Hybrid Simulation of the DRAMA Radio and Line-of-Sight Multipath Channel	C-1
D Synopsis of Selective Fading Test and Evaluation for Digital LOS Channels	D-1



## LIST OF ILLUSTRATIONS

<u>Figure</u>	<u>Title</u>	<u>Page</u>
1.	YEARLY DISTRIBUTION OF K FACTOR FOR THE PHILIPPINES	6
2.	PATH PROFILES FOR VARIABLE K FACTOR (K = 0.34, 0.5, AND 0.67)	7
3.	PATH PROFILES FOR VARIABLE FRESNEL CLEARANCE AND K = 0.67 (F = 0.3, 1.0, 2.0 and 11.0)	8
4.	PATH PROFILE FOR VARIABLE FRESNEL CLEARANCE (F = 3.0, 4.0, 5.0, AND 11.0) AND K = 1.67	9
5.	'M' AMPLITUDE VS PATH LENGTH DIFFERENCE VS VARIABLE K FACTOR AND TIDE HEIGHT	11
6.	TIME DELAY VS PATH LENGTH DIFFERENCE FOR VARIABLE K FACTOR AND TIDE HEIGHT	12
7.	'M' AMPLITUDE VS PATH LENGTH DIFFERENCE FOR K = 0.65	13
8.	TIME DELAY VS PATH LENGTH DIFFERENCE FOR K = 0.65	14
9.	DEGRADATION IN SIGNAL-TO-NOISE RATIO VS DELAY FOR SIMULATION OF DRAMA RADIO	16
10.	ANTENNA HEIGHT VS AVAILABILITY FOR K < 1 (BASED ON METEOROLOGICAL DATA)	18
11.	'F' AMPLITUDE VS PATH LENGTH DIFFERENCE FOR VARIABLE K FACTOR AND TIDE HEIGHT	20
12.	'F' AMPLITUDE VS PATH LENGTH DIFFERENCE FOR K = 0.65	21
13.	SURFACE DUCTING EFFECTS	22
14.	ATTENUATION DUE TO PRECIPITATION (AFTER CCIR)	23
15.	EXAMPLE OF EP 27-77 LINK PERFORMANCE CALCULATIONS	26
16.	TYPICAL RADIATION PATTERN OF A 12 FT. CIRCULAR PARABOLIC ANTENNA	30

## LIST OF TABLES

<u>Table</u>	<u>Title</u>	<u>Page</u>
I.	EXPECTED FREQUENCY SELECTIVE FADING OF MANILA EMBASSY-SANTA RITA LINK	17
II.	SUMMARY OF EXPECTED PERFORMANCE DEGRADATION CAUSED BY FADING MANILA EMBASSY-SANTA RITA DIGITAL LOS LINK	25
III.	ALTERNATIVES FOR MANILA EMBASSY-SANTA RITA DIGITAL LOS LINK CONFIGURATION	28

## I. INTRODUCTION

The purpose of this analysis is to assess performance of the digital LOS radio link between the U.S. Embassy in Manila and Santa Rita, Republic of the Philippines, and to provide technical guidance for an optimum implementation of this link in accordance with DCS performance standards.

DCA PAC as a result of concern over the degradation in performance of the radio link tasked DCEC to study the link and develop alternatives for improving the performance. A detailed account of correspondence involving the study is given in Section II, Background. The link performance analysis is described in detail in Section III, and recommendations for an optimum link design given in Section IV. The analysis is concluded in Section V, followed by a list of references and additional technical information contained in Appendixes A to D.

## II. BACKGROUND

Abnormal propagation conditions, excessive path length and inadequate path clearance at the reflecting point in the vicinity of the Manila Embassy end were identified by NAVSEEA PAC (Msg 280049Z, December 1976 and TEP Report of April 1977) as major sources of excessive RSL fading (over 40 dB at times) on analog link M1433.

DCA PAC (Msg 302033Z, April 1980) expressed concern over degradation in the performance of DRAMA radio equipment due to the multipath fading conditions on the subject link. Two alternatives employing coherent IF combining, adaptive equalization (AE) and space diversity (SD) were recommended to DCEC for evaluation.

The host government (HG) authorities recommended the following frequencies on the subject link (NAVSEEA PAC Msg 2301180Z, June 1980): 7635.35 MHz for the Embassy to Santa Rita link, and 7412.5 MHz for the Santa Rita to Embassy link; ECAC (Msg 161440Z, July 1980) evaluated the new frequencies and found them compatible.

In reply to the DCA PAC request of April 1980, DCEC (Msg 301739Z, June 1980) reviewed the "in-house" R&D program related to analysis of frequency selective fading (FSF) effects on digital LOS links, scheduled preliminary results of the analysis, and expanded alternatives to include a quad-diversity (QD) configuration, or addition of an active repeater at Angat.

The alternative of adding an active repeater at Angat was ruled out by DCA PAC (Msg 080053Z, July 1980) and NAVSEEA PHILIPPINES (Msg 142230Z, July 1980) as being operationally unacceptable due to the requirement for expansion of the building at Angat, the possibility of path obstruction by future high-rise construction, and reduction in survivability. Information on quad diversity was provided by DCEC (Msg 231811Z, July 1980).

Results of the preliminary analysis (1 August 1980) were presented by the DCEC action officer during the PAC area visit of 21-31 August 1980. The results indicate possible substandard performance caused mostly by variation in K factor (subrefractive) and negligible degradation due to frequency selective fading (FSF). A recommendation was made to raise the antenna height at the Embassy location and employ SD in lieu of programmed frequency diversity (FD) configuration. A follow-up message (291443Z, October 1980) reiterated the findings of the preliminary analysis, recommended a change in procurement in DRAMA radio equipment (i.e. AN/FRC-171 instead of AN/FRC-173), and indicated no significant performance advantage to be gained with radio equipment employing adaptive equalization.

DCA PAC (Msg 171953Z, November 1980) and NAVSEEA PAC (Msg 042314Z, November 1980) requested additional information on the analysis, assumptions, and rationale for using SD and not using AE, and questioned the validity of results based on Clark AB meteorological data.

The distinction between multipath flat fading versus frequency selective fading and the appropriate corrective actions were contained in DCEC replies (Msgs 181911Z, November 1980 and 011333Z, December 1980) to messages of the preceding paragraph. It also requested data to characterize type and magnitude of fading affecting performance of the existing analog link to be considered in the final analysis.

In reply to the DCA 471 request on the impact on the PDU program (Msg 042047Z, November 1980), DCA PAC indicated (Msg 092113Z, December 1980) that DRAMA radio equipment could not be used unless AE would be available by August 1982, requesting a confidence level for such a deadline. DCA also reiterated findings of NAVSEEACTION PHIL (Msg 080430Z, August 1980) that the antenna tower at the Manila Embassy would not support the additional antenna required for an SD or QD configuration.

A DCA/DCEC reply (Msg 162045Z, December 1980) recapitulated information from previous DCEC messages, indicated that a review of data on-hand showed evidence of flat fading and no FSF, thus precluding use of AE, expected to be available in 2-1/2 years. It stated that for a fixed K factor of 2/3, DCS performance standards are met with subject LOS link configured in FD with 15 foot antennas, or SD with 12 foot antennas, or SD with 10 foot antennas and low noise preamplification. The reply suggested another look at the addition of another antenna on the embassy tower to accommodate the SD configuration.

COMNAVTELCOM estimated a two-year delay in schedule if procurement of the DRAMA radio equipment was changed to SD instead of FD, and requested COMNAVEXSYSCOM to proceed with FD and investigate using smaller antennas in SD at Manila (Msg 291657Z, December 1980).

The DCEC final analysis (Msg 071629Z, April 1981), which confirmed preliminary results, summarized results of two digital LOS link tests showing negligible effects of FSF on link performance and recommended an SD configuration with a 12 foot antenna. It further recommended 3 to 6 months of in-service monitoring to determine/optimize link performance with the possibility of reorienting the antenna boresight to compensate for the subrefractive K factor.

The results of a structural analysis performed by NAVSEEACTION PHILIPPINES (Msg 200215Z, May 1981) showed that the existing 105 ft. tower at the Manila Embassy would not support an additional 15 foot antenna, and recommended a new antenna tower.

COMNAVTELCOM requested NAVSEEACTION PHILIPPINES (Msg 082017Z, June 1981) that cost estimates for the new tower at the Embassy include both options: (1) FD with a 15 foot antenna, (2) SD with two 12 foot antennas.

NAVSEEACTION PAC study on various types of diversity (Ltr of 17 April 1981) recommended a hybrid diversity system (SD at Santa Rita and FD at the Embassy) as a compromise link configuration.

### III. LINK PERFORMANCE ANALYSIS

The expected performance for the upgraded and cut over Manila Embassy - Santa Rita link is assessed in terms of link availability and channel quality criteria described in DCEC TR 12-76, "DCS Digital Transmission System Performance," November 1976. The design procedures for LOS digital transmission systems contained in DCEC EP 27-77, "Design Objectives for DCS LOS Digital Radio Links," December 1977 were followed in this analysis with emphasis on the areas of concern identified below.

#### 1. AREAS OF CONCERN

The following areas of concern are addressed in this performance analysis, most of which were identified in the extensive correspondence reviewed in section II:

- a. Yearly variation of K factor.
- b. Path clearance required for corresponding K factors.
- c. Performance degradation caused by normal fading conditions (multipath, absorption and fog).
- d. Performance degradation caused by abnormal fading conditions (variable K factor, ducting and rain).
- e. Path loss calculations accounting for contributions of areas c. and d.
- f. Expected link performance considering improvements gained through diversity configuration, larger antenna size and boresight reorientation, low noise preamplifier and other equipment.
- g. Link design and activities selected to achieve optimum performance on a cost-efficient basis.
- h. Improvement in link performance gain by using non-DRAMA radio equipment with an adaptive equalizer.

#### 2. YEARLY K FACTOR DISTRIBUTION

The most recent publications dealing with the weather conditions, meteorological data and distribution of the refractivity gradient data ( $dn/dh$ ) typical of the Central Luzon Island area were reviewed in order to determine the K factor distribution characteristic of the subject link. The refractivity gradient data shown for the Clark Field, Luzon area in reference [1], were used, following the technique described in Appendix A to derive the K factor distribution curve shown in Figure 1. The error introduced by using the Clark Field data (~50 miles NW of Manila) instead of either end location is insignificant, when compared with equivalent empirical data depicted in reference [2]. Note the subrefractive characteristics (i.e.,  $K \ll 1$ ) of the K

factor governing the subject link throughout most of the year. An average K factor of  $\approx 0.35$  was measured by USNEL [2] at both the Santa Rita and Manila Embassy locations during the February-April months (dry season). The rainy season, extending from May to December, is characterized by frequent and heavy precipitation. The variations in the propagation media of the subject link all controlled mostly by the high humidity and frequent temperature inversions during the dry season months (January-April), and to a much smaller extent by the local precipitations of the wet season (May-December). Their impact on the link performance is assessed in the path clearance (subsection 3.) and path loss/fade margin (subsection 6.) calculations.

### 3. PATH PROFILES

A set of path profiles presented in this section is based on the variations in the propagation media calculated in the previous section, and on the previous test results/analysis performed by NAVSEEACTION FAC on the existing analog link connecting the same end locations. The most stringent values controlling such variations range from the subrefractive K factor distribution (Figure 1) to the multi-Fresnel zones (up to 12) mentioned in the NAVSEEACTION PAC analysis. DCEC PFLOS program is used to plot the path profiles shown in Figures 2-4. The path profiles of Figure 2 depict the relationship of the antenna tower height at the Embassy to the minimum path clearance required for subrefractive values of  $K = 0.34, 0.5$ , and  $0.67$ , and a fixed Fresnel clearance of  $0.3$ . Note that the height of the existing tower (26 meters, i.e., 85 feet) at the Embassy would satisfy the minimum path clearance for  $K = 0.67$  and  $0.3$  F, but not for smaller K values. An antenna tower height of 152 meters would be required for the path clearance corresponding to  $K = 0.34$  and  $0.3$  F. The set of path profile curves shown in Figure 3 depicts the path clearance relationship corresponding to a fixed K factor of  $0.67$  and a wide variation in the Fresnel zones ranging from  $0.3$  F to  $11.0$  F. Note that partial or total path blockage results for Fresnel zones higher than  $1.0$  F. The path profiles of Figure 4 show the same variation in the Fresnel zones for a K factor of  $1.67$ , where an adequate path clearance is obtained with Fresnel zones up to  $3.0$  F.

Therefore, the existing antenna heights would meet the minimum path clearance criteria for any combinations of K and F values ranging from  $K = 0.67/2.0$  F to a  $K = 1.67/3.0$  F. Any other mix of K and F values outside this range would require a proportionate increase in antenna tower height(s).

### 4. PERFORMANCE DEGRADATION CAUSED BY NORMAL FADING

In general, the performance of a LOS link is defined in terms of the characteristics of atmospheric conditions above the path of propagation. Variations in the received signal strength (RSL) are caused by fading, usually a combination of various normal and abnormal types of fading. The normal fading occurs a large percentage of time, with a predictable (90-95%) behavior and occurrence. Cause include the following: (1) atmospheric multipath, which could be either flat (all frequencies) or frequency selective (only specific frequencies); (2) atmospheric absorption; (3) fog; and (4) dust.

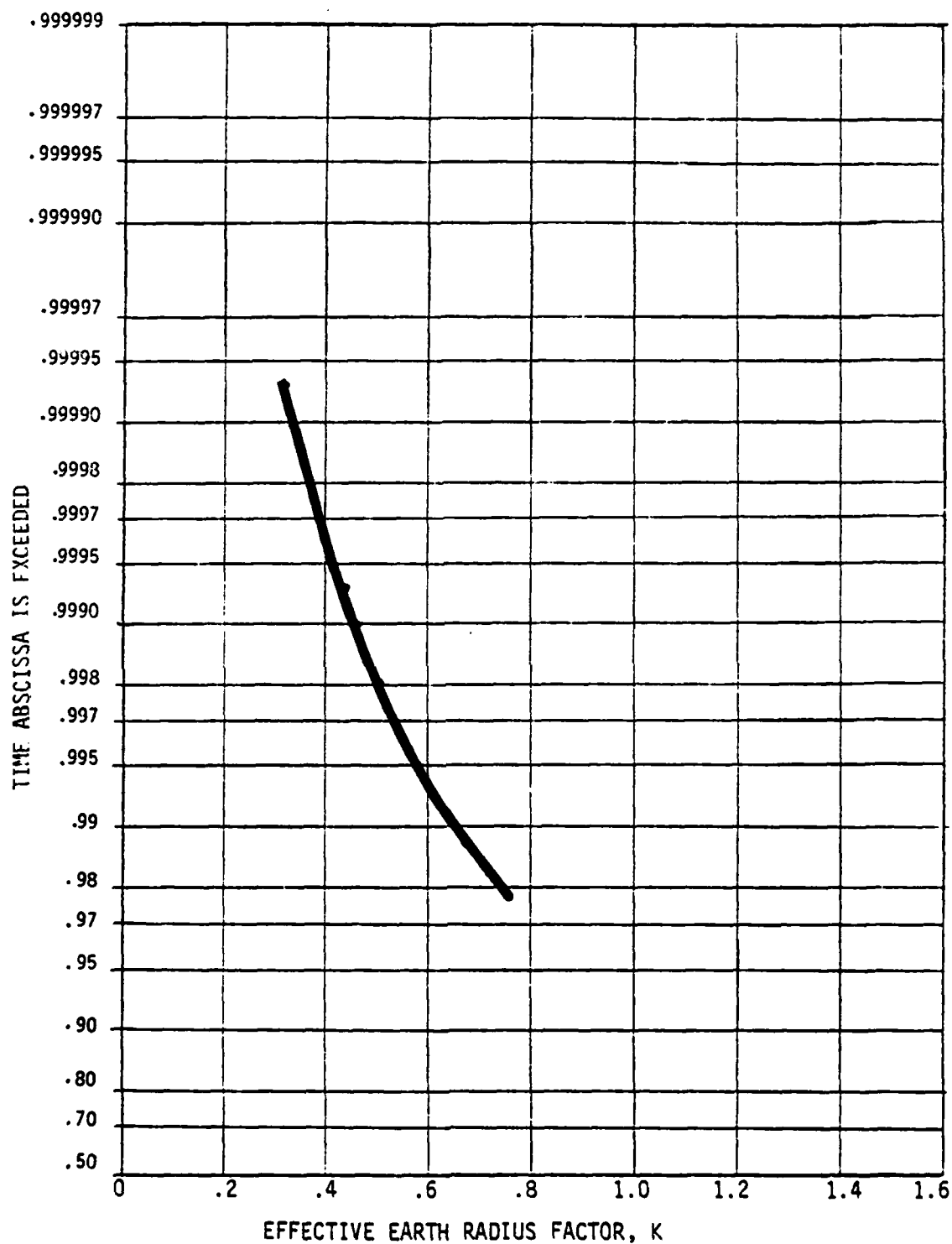
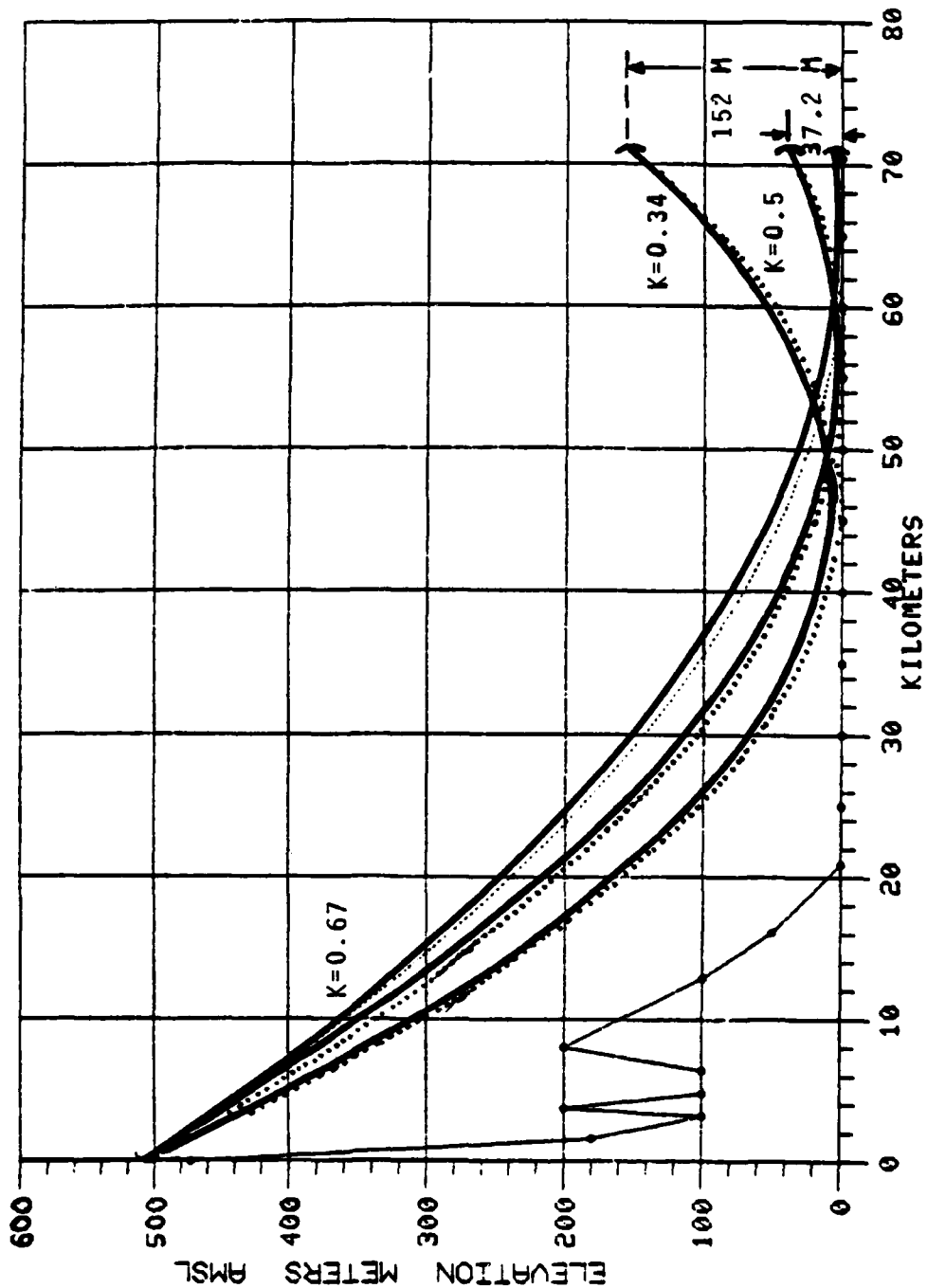


Figure 1. Yearly Distribution of K Factor for the Philippines





PATH PROFILE FOR LINK : M1433  
 DATE: 16-MAY-80

Figure 2. Path Profiles for Variable K Factor  
 (K = 0.34, 0.5, and 0.67)

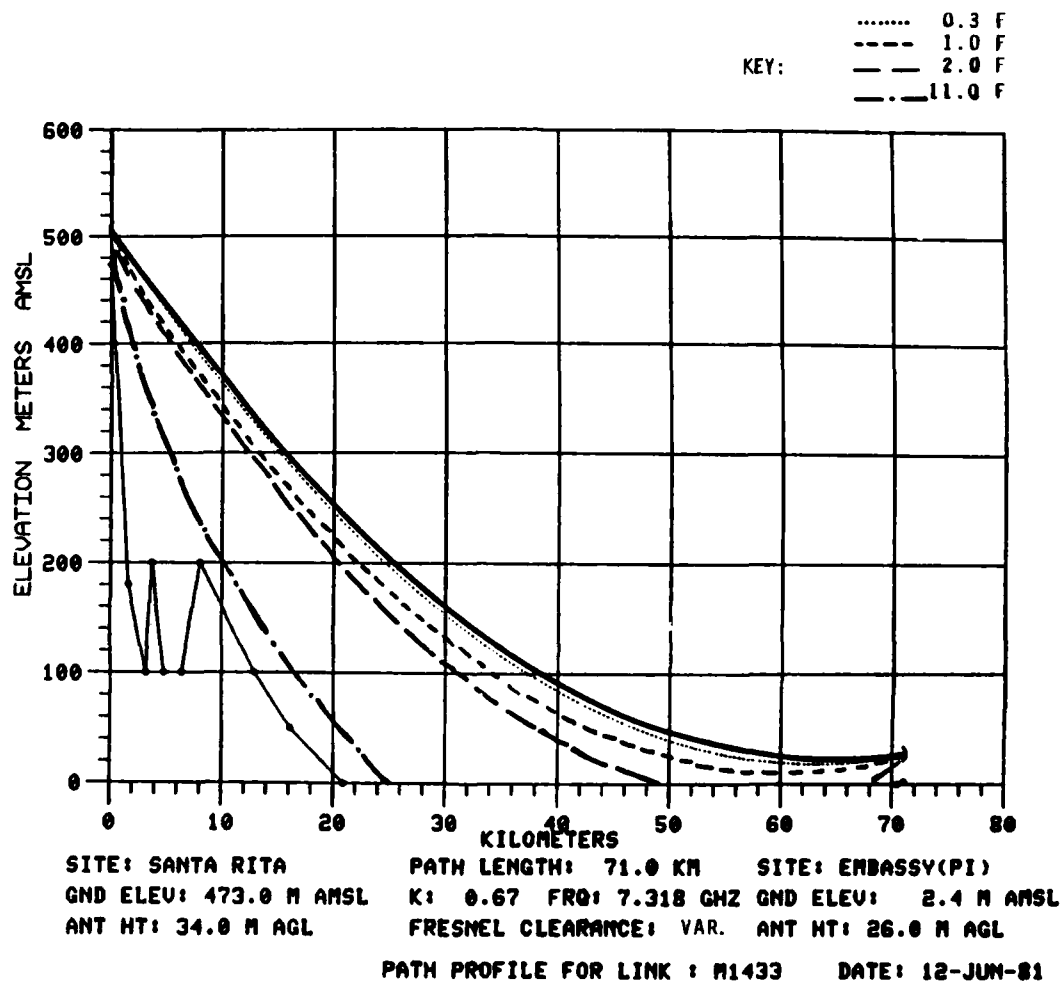


Figure 3. Path Profiles for Variable Fresnel Clearance and  $K = 0.67$   
 ( $F = 0.3, 1.0, 2.0$  and  $11.0$ )

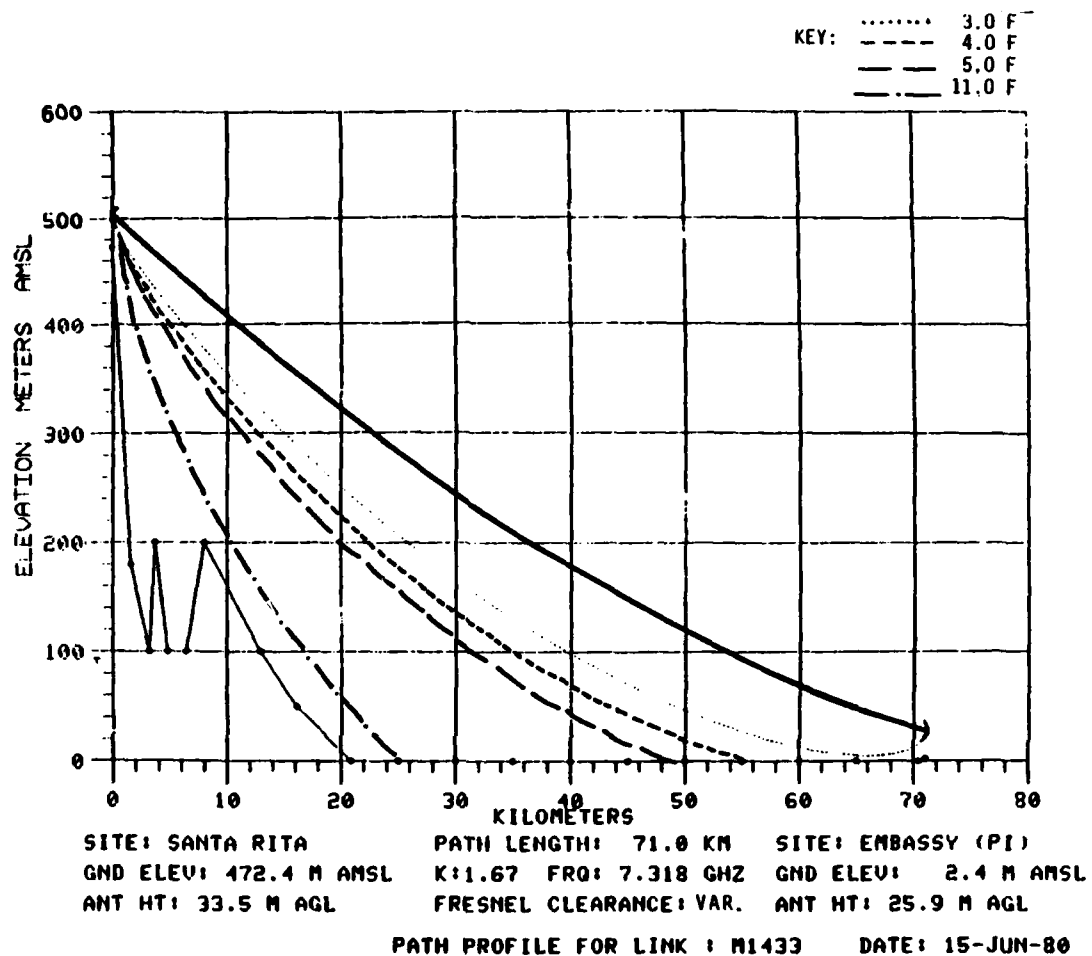


Figure 4. Path Profile for Variable Fresnel Clearance  
 (F = 3.0, 4.0, 5.0, and 11.0) and K = 1.67

The effects of multipath are considered in this section; the other effects make a negligible contribution to the link performance.

a. Multipath Flat Fading. The LOS link design of EP 27-77, "Design Objectives for DCS LOS Digital Radio Links," December 1977, describes this type of fading and relates it to the DCS performance criteria through applicable outage types and related probabilities. A link margin ( $M_L$ ) design objective of  $M_L = 9 \log D + 18$  in dB ( $D$  = path length in km) is used in conjunction with path clearance criteria of  $K = 2/3$  and  $0.3 F$  to meet such a criterion. This results in a link margin of ~35 dB for the case of average climate, terrain, and temperature using dual space diversity (with vertical antenna separation of 9 meters).

Results of previous tests run on an existing link reported in the Technical Evaluation Report (TEP) of 1977 and message correspondence of NAVSEACT PAC (see section II) have indicated attenuations in RSL ranging from 30-40 dB, most of the drop being caused by multipath fading. The present analog configuration employs dual frequency diversity and is sized for a 120 voice channel capacity.

b. Multipath Frequency Selective Fading. This section addresses the most disputed area of concern (refer to summary of correspondence in section II) - the multipath frequency selective fading (FSF).

A computer program was developed in support of the FSF analysis to calculate path length difference versus power ratio and time delay variations. The program is based on a two-ray channel model, comprising a direct signal path versus a reflected/refracted signal path. A description of these program calculations, supporting subprograms, and an example of the results is presented in Appendix B. The program has been "customized" to the subject link, but it can be used for any other LOS link depending on the availability of input parameters. This program takes into account the following parameters: (a) various antenna heights at Santa Rita (1660-1550 feet, in steps of 10 feet), (b) changes in tide heights at the reflection point (4 to -1 foot, above mean sea level (AMSL) by 1 foot increments), and (c) different values of K factor (ranging from 0.55 to 2.0).

The results of this program are summarized in Figures 5 through 8. The path length difference ( $\Delta R$  in feet) versus the ratio of the reflected signal path amplitude to the direct signal path amplitude ( $M$  in dB) is shown in Figure 5 for variable tide and K factor, or for  $K = 0.65$  as shown in Figure 7. The time delay (DTM in nanoseconds) versus path length difference ( $\Delta R$  in feet) relationships for a variable K factor and for  $K = 0.65$  are shown in Figure 6 and Figure 8 respectively. Note the maximum value of  $M$  for  $K \geq 0.83$  (Figure 6) and the negligible effect on  $\Delta M$  caused by variation in tide height (Figure 7). Also of significance is the steep increase in DTM for  $K > 0.65$  (Figure 6), and the fact that tide height variation has no effect on DTM (Figure 8).

The values of the power ratio and delay of the two-ray signal path are used for inputs to the hybrid simulation of the DRAMA radio and a LOS fading

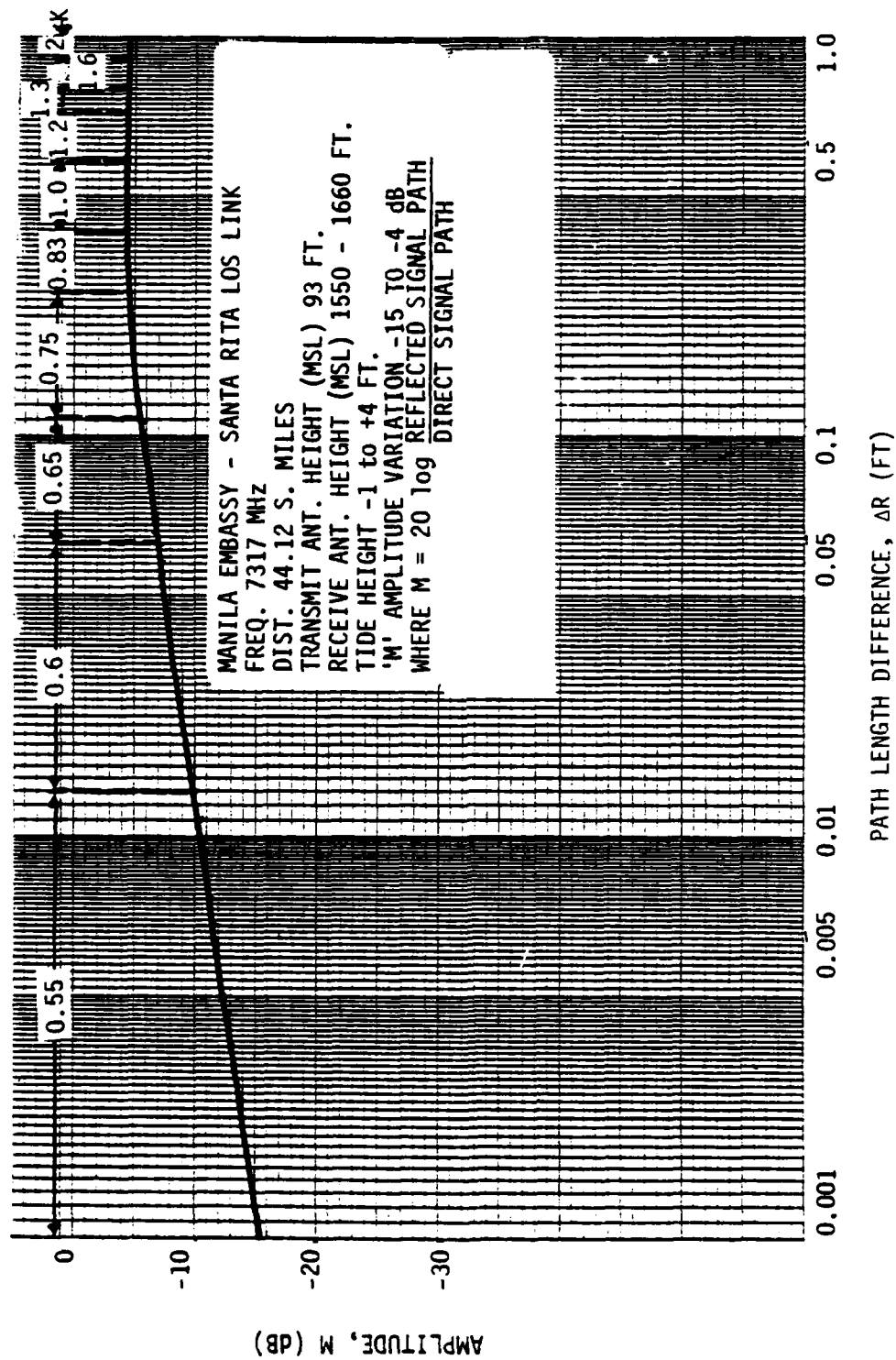


Figure 5. 'M' Amplitude vs Path Length Difference vs Variable K Factor and Tide Height

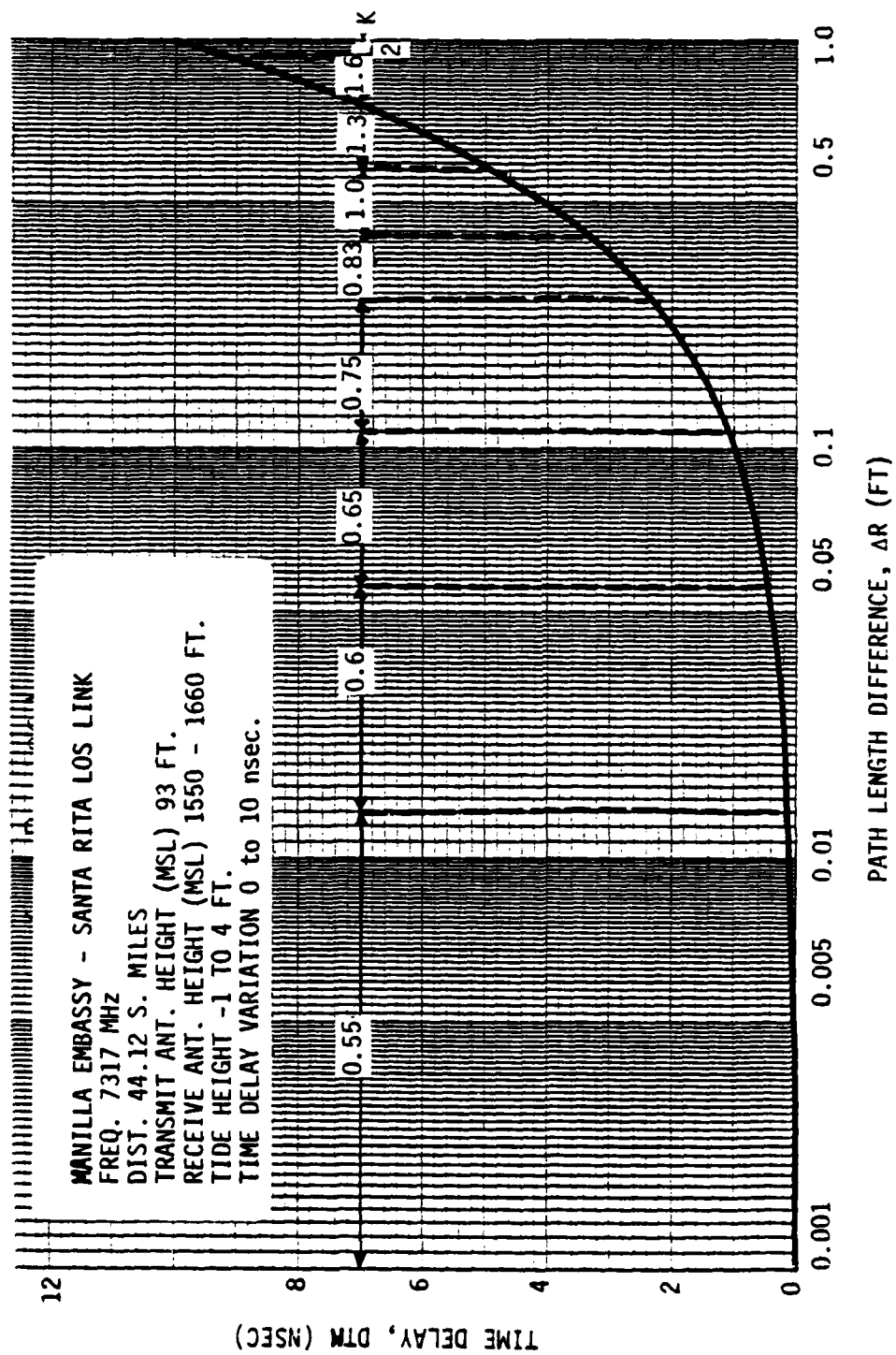
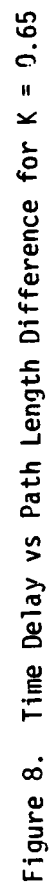


Figure 6. Time Delay vs Path Length Difference for Variable K Factor and Tide Height







channel described in Appendix C. Performance degradation caused by FSF is assessed from the yearly distribution of the K factor shown in Figure 1, the variation in amplitude (M) and delay (DTM) depicted in Figures 5 and 6, and other input parameters for the hybrid simulation specific to the DRAMA radio equipment and the LOS channel characteristic of the link. The family of curves of Figure 9 illustrates the results of this simulation. Degradation in the SNR required for a  $10^{-3}$  BER is related to the time delay (measured in bit times) and various power ratio values ( $1/2 < \alpha < 1/8$ ). A summary of the degradation in performance caused by FSF expected on the subject LOS link is presented in Table I. Note that with the small delay values, approaching zero, there is a gain in SNR, resulting from constructive (rather than destructive) interference of the two signal rays. Hence, for a  $K = 0.67$ , a SNR improvement of 1.5 dB results from the simulation of the DRAMA radio. For higher values of delay, the degradation in SNR ranges from 3 ( $K = 1$ ) to 4 dB ( $K = 2$ ). The FSF changes in SNR listed in Table I were assessed for a single diversity mode. Improvements in SNR performance from diversity combining and the capability of diminishing FSF effects of various radio combiner/switching configurations have been documented as described in Appendix D.

##### 5. PERFORMANCE DEGRADATION CAUSED BY ABNORMAL FADING

Abnormal fading occurs a small percentage of time, with an unpredictable behavior and occurrence. The following types are included under this category: (1) subrefractive ( $K < 1$ ), (2) superrefractive ( $K > 1$ ), (3) ducting, and (4) rain attenuation. The geographical location, topography, climate and weather conditions indicate that all four types of abnormal fading affect the performance of the subject link. This subsection deals with each of these propagation impairments and assesses their performance degradation.

a. Sub- and Superrefractive Fading. A wide variation in the refractivity gradient ranging from subrefractive ( $K < 1$ ) to superrefractive ( $K > 1$ ) conditions during the wet season months (May-December) was reported in both references [1] and [2]. The more critical of these two types of fading is the subrefractive condition which causes an inadequate path clearance (or earth bulge). Figure 10 illustrates the relationship between availability and antenna heights for variable K factor values using the yearly distribution of Figure 1. Note that partial or total path blockage would result for decreasing K factor values when availability is evaluated for the existing antenna tower heights. An antenna height of 134 meters (442.2 feet) would be required at the Manila Embassy location for an adequate path clearance satisfying the most stringent K factor ( $K = 0.35$ ) calculated from the available meteorological data. Obviously an increase of over 100 meters (330 feet) in the antenna height is not a viable solution. The super-refractive fading arises from variations in K factor toward the maximum values, which are expected to exceed a value of 1.33 ( $K \geq 4/3$ ) in about half the time (reference to yearly distribution of Figure 1).

Utilizing the "two-ray model" described above, the variation of the signal strength in relation to the K factor is derived for the subject link. Figure 11 shows the variation in path length difference ( $\Delta R$  in feet) with respect to

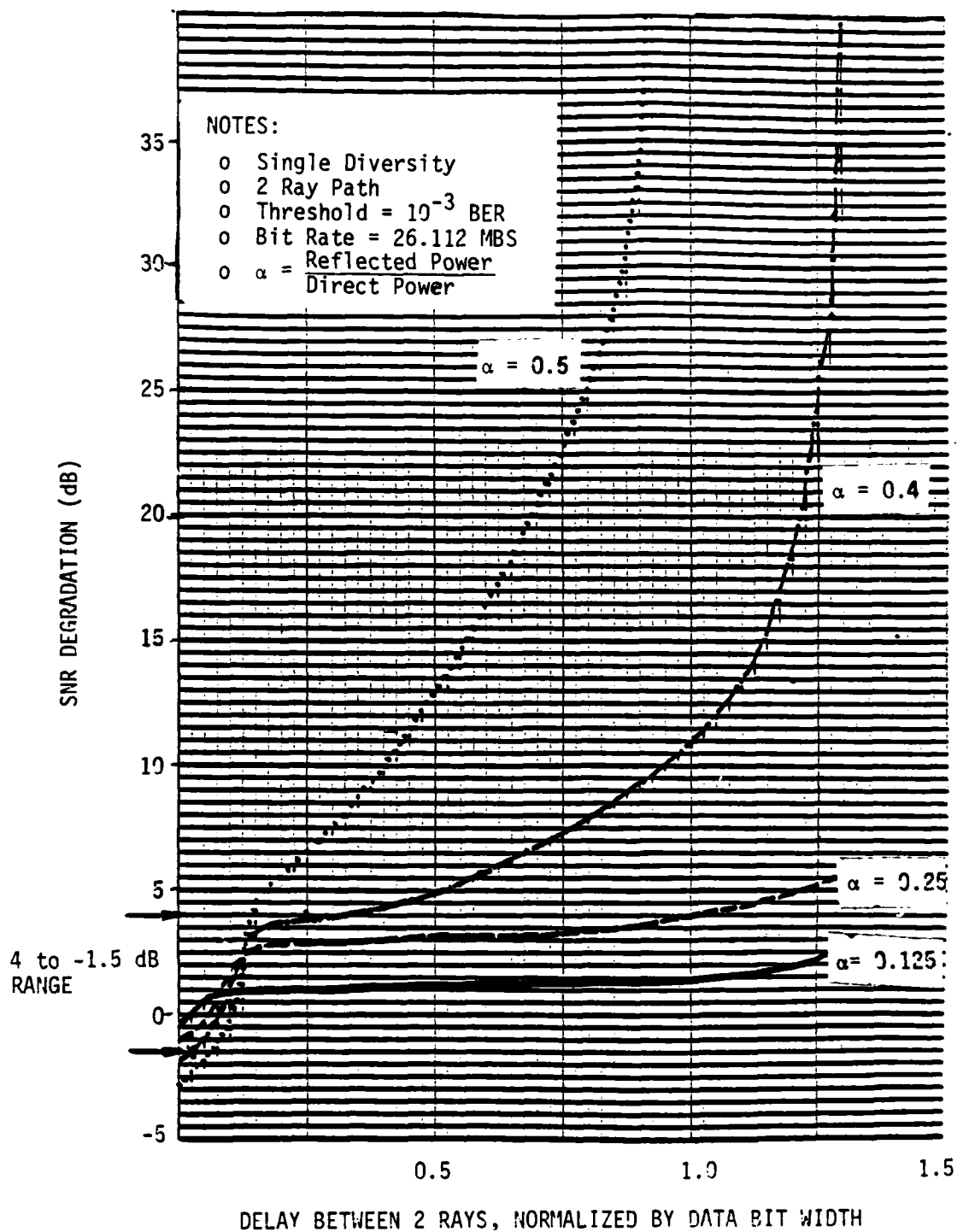


Figure 9. Degradation in Signal-to-Noise Ratio vs Delay for Simulation of DRAMA Radio

TABLE I.

## EXPECTED FREQUENCY SELECTIVE FADING OF MANILA EMBASSY-SANTA RITA LINK

K FACTOR (FIG. 1)	TIME EXCEEDED (FIG. 1)	AMPLITUDE RATIO-M (FIG. 5)	POWER RATIO- $\alpha$ (NOTE 1)	TIME DELAY-DTM (FIG. 6)	DELAY, IN BIT WIDTHS (NOTES 2&4)	SNR DEGRADATION (FIG. 9)
0.67	0.985	0.56	0.32	1 nsec	0.026	-1.5 dB
1.0	0.9 (Note 3)	0.63	0.4	5 nsec	0.13	3 dB
1.33	0.5 (Note 3)	0.63	0.4	7 nsec	0.18	3.5 dB
2.0		0.63	0.4	10 nsec	0.26	4 dB

- NOTES: 1.  $\alpha \propto \Delta M^2$
2. Delay  $\Delta$  DTM x Bit Rate (For QPR)
3. Extrapolated Value
4. Bit Rate = 26 Mbs

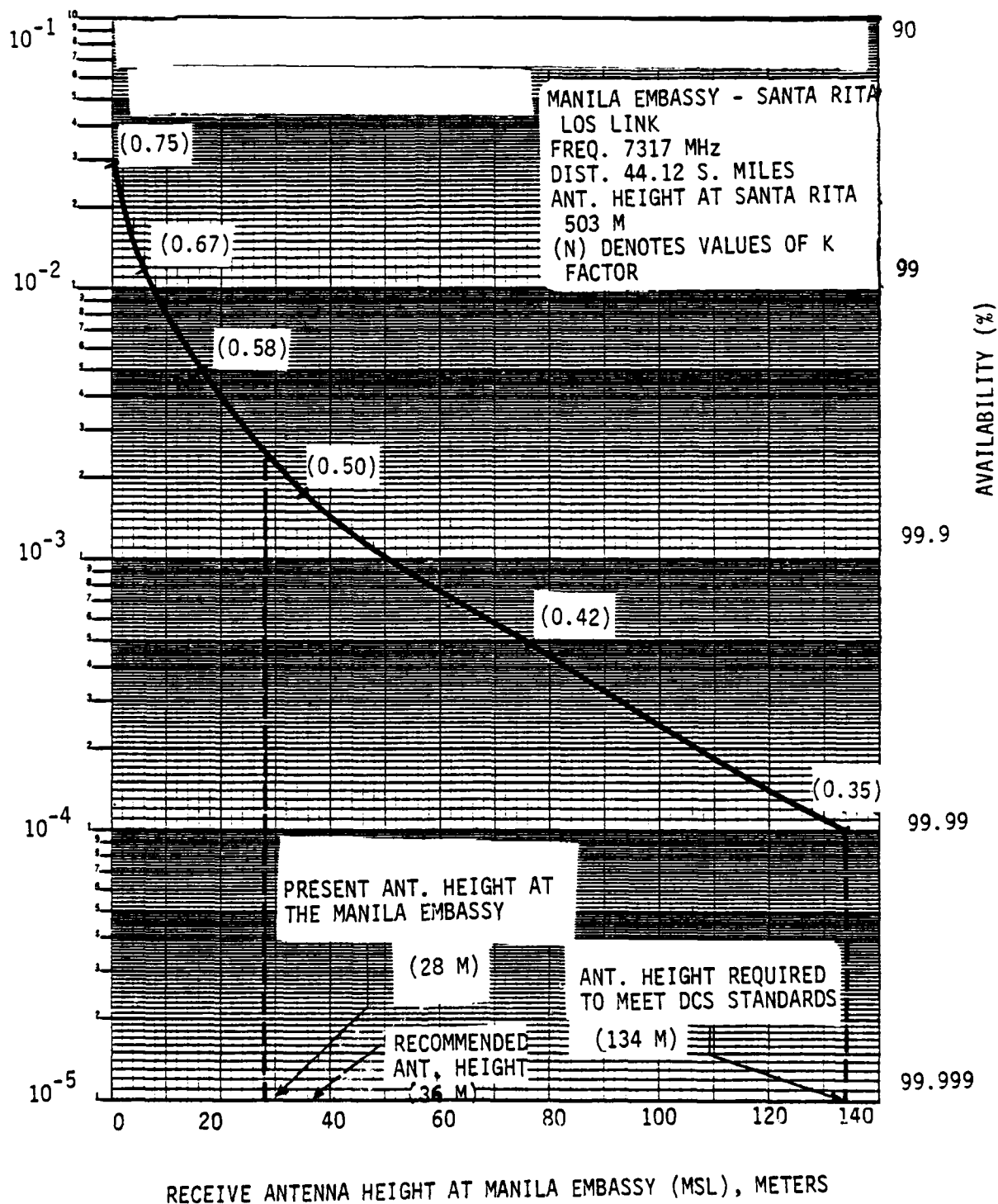


Figure 10. Antenna Height vs Availability for  $K < 1$   
(Based on Meteorological Data)

the ratio of the resultant path to direct signal path (F in dB) for a K factor ranging from 0.55 to 2.0, a tide height of -1 to 4 feet, and an antenna height at Santa Rita varying from 1550 to 1660 feet. The same relationship for a fixed  $K = 0.65$  is shown in Figure 12. Note in Figure 11 the numerous Fresnel zones (15) within a K factor variation of  $0.55 < K < 2.0$  where the signal ratio ranges from a maximum value of 4 dB down to a minimum of -8.5 dB. Also note the negligible effect of tide height variation shown in Figure 12. Furthermore, the efficiency of space diversity (antennae spaced 33 feet apart) and optimum antenna heights in relation to the even Fresnel zone nulls are depicted in these two figures.

Experience gained through the design and performance of other DCS LOS paths has indicated that the effective K factor over the entire path reaches a minimum ( $K = 0.3$  in Figure 1), or a maximum ( $K = 2.0$  in Figure 11), value for a much smaller percentage of time than would be indicated by the distribution of K value as found by meteorological measurements at single points. The explanation given in reference [3] is that the unusual conditions causing these extreme values are unlikely to occur over more than a small part of the path at any given instant. Hence the analysis of this link considered variations in K factor ranging from 0.5 to 2.0, and a median, or "normal", of 0.67.

b. Ducting. Surface ducting caused by a combination of super-refractivity, heavy humidity layering, and sudden temperature inversions that prevail during the dry season months (January-April) has been identified in reference [2] as the major cause for deep fading in the RSL of the subject link. The worst fading conditions occurred during mid-April, between 0800 and 1600-2200 hours of the day, with a wide fade duration of several minutes (10 or less) when the RSL dropped from 15 dB (2-5 minutes) to more than 25 dB (less than a minute). Such a fade distribution was measured at the Manila Embassy terminal, at a 152 foot elevation using a frequency of 1745 MHz (reference [2]). An additional 12.5 dB in this fading distribution ( $20 \log (7.318-1.745)$ ) is expected for the median frequency of 7.318 GHz. The effects of surface ducting are shown in Figure 13. The path profile of the preliminary BESEP [4] was used for a better illustration of the signal path, earth bulge and ducting effects. Note the reflection of the signal and the disruption of signal paths (both direct and sea-reflected) caused by the surface duct layer.

c. Rain Attenuation. The weather during the rainy season (May-December) has been characterized (in reference [2]) "by frequent and heavy precipitation, much of each is the result of a local squall condition rather than the passing of large frontal air masses. Frequent rain tends to mix the air of the lower atmosphere, reducing the probability of stratification".

The magnitude of rain attenuation is controlled mostly by the maximum instantaneous intensity of the rainfall, and the size of the area over which the high intensity (rain) cell extends at any given moment. Very little information on these two entities is available for the subject link; thus the rain attenuation is a probabilistic estimation. The attenuation due to precipitation (CCIR model) is shown in Figure 14. Accounting for the

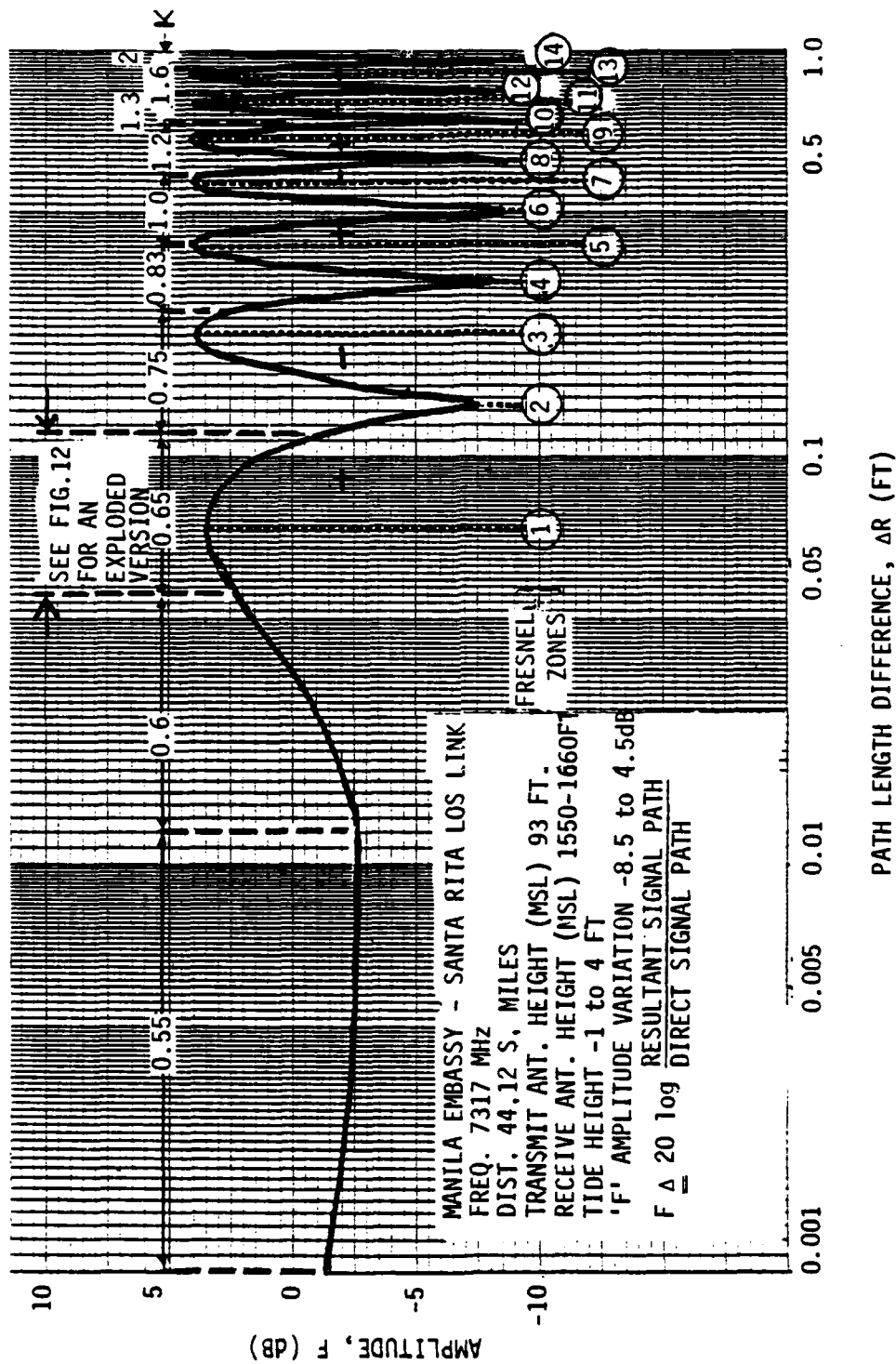


Figure 11. 'F' Amplitude vs Path Length Difference for Variable K Factor and Tide Height



# PATH PROFILE ANALYSIS

Local Station: Santa Rita  
 Site Elevation: 1550 Feet  
 Antenna Height = 110 Feet

Distant Station: Embassy  
 Site Elevation = 8 Feet  
 Antenna Height = 85 Feet

Path Length = 44.12 Miles  
 Earth Curvature Factor,  $K = 2/3$   
 Mean Frequency = 7317.5 MHz

Legend:  
 - - - Direct Ray  
 - - - B.3 Fresnel Zone  
 - - - Reflection (At Sea Level)  
 ↑ Tree  
 | Man Made Obstacle

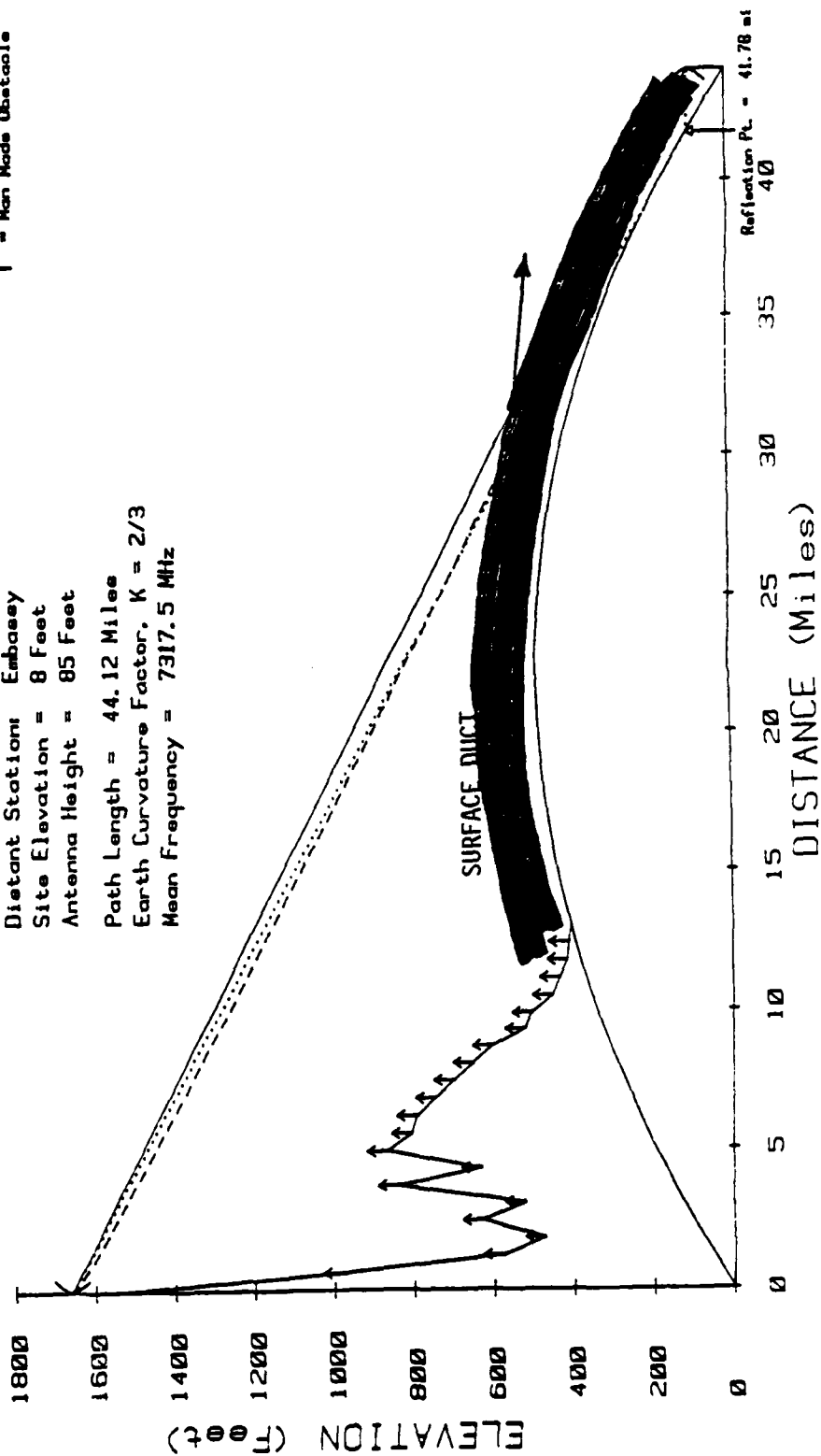


Figure 13, Surface Ducting Effects



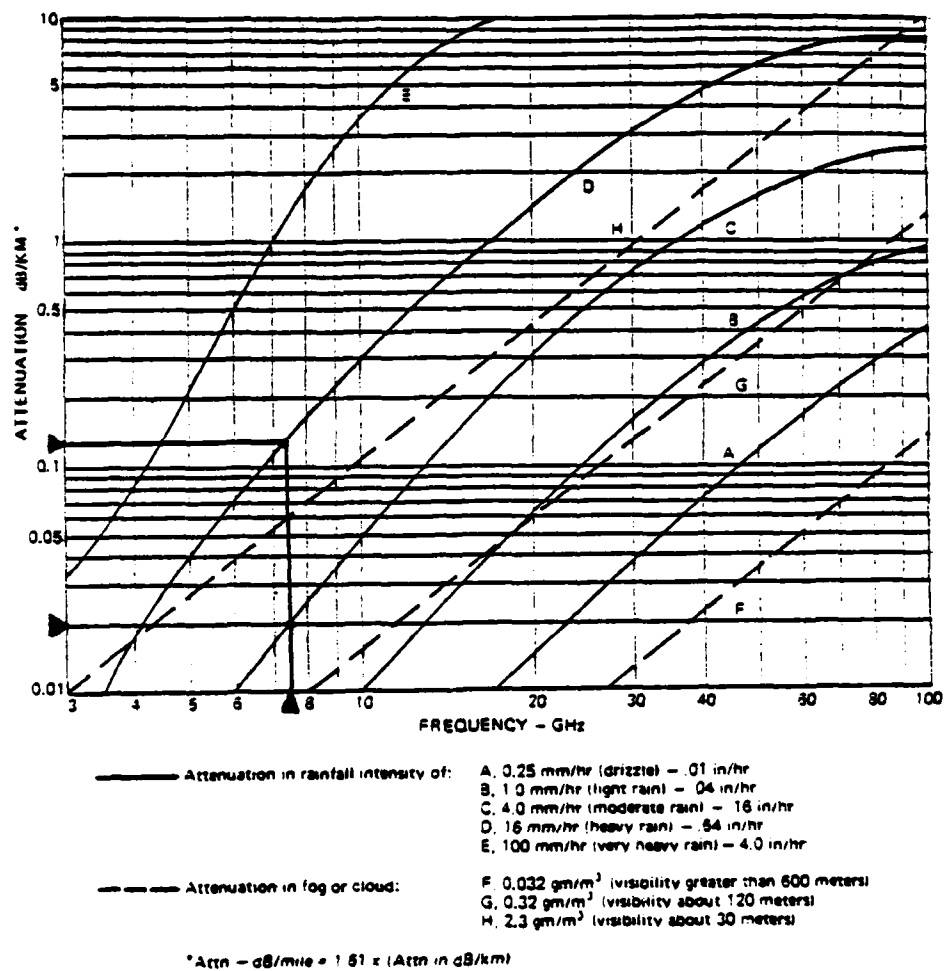


Figure 14. Attenuation Due to Precipitation (After CCIR)

intensity and area of precipitation reported for the rainy season, the rain attenuation could vary from 2 to 10 dB (see arrows in Figure 14). Note that, since negligible multipath fading and ducting occur during periods of heavy rainfall, most of the fade margin is available to combat the rain attenuation.

## 6. SUMMARY OF EXPECTED PERFORMANCE DEGRADATION

The various types of fading expected that affect the performance of subject link are summarized in Table II. The magnitude (in dB) of degradation and corrective actions designed to alleviate such effects are tabulated for each type of fading considered in this section. The expected or measured rate of occurrence for each type of fading is listed in the "Remarks" column.

In general, a combination of normal fading (predictability  $\approx$  90 to 95% of time) with a specific type of abnormal fading (predictability  $\approx$  1-5% of time) would characterize the propagation conditions and in turn, the link performance. Such a fading mix includes: multipath plus sub-refractive or super-refractive fading, multipath plus surface ducting, and others. At the same time, some of the fading occurrences are mutually exclusive, such as: multipath or ducting that would not occur during rain attenuation fading, and sub-refractive that would exclude super-refractive fading. It would be a formidable task to determine their distribution in relation to time and location along the path. Instead, the major contributors to link performance degradations are analyzed and corrective actions are recommended to diminish their effects on overall path reliability.

## 7. EXPECTED LINK PERFORMANCE

A closer review of Table II indicates that the atmospheric anomalies which will probably cause degradation of system performance most of the time on the Manila Embassy-Santa Rita digital LOS link will be a combination of multipath flat fading and surface ducting. These have been reported [2] to occur during the month of April, when the atmospheric conditions are characterized by surface layering of high humidity causing above-standard gradients (low K factor) and abrupt temperature inversions. Depending on the duration and location of such adverse atmospheric conditions, the performance of the subject link could be degraded to the level of complete outages that are repetitive (less than 10 deep fades per day) and each lasting a very short time (few seconds). Use of space diversity would alleviate the effects of this type of fading combination. Also, depending on the thickness and height of the ducting layer, a slight upward offsetting in the bore angle of the upper antenna at the Manila Embassy would further increase the link performance. The same link design approach would diminish degrading effects caused by another fading combination - flat multipath with sub-refractive fading.

Design trade-offs among specific parameters of major components affecting link performance (such as diversity, antenna size and bore angle, transmitter output power, receiver noise figure) are reviewed in order to optimize performance at a minimum cost. An example of link performance calculations using the EP 27-77 computer program is shown in Figure 15. For a dual space

TABLE II.  
SUMMARY OF EXPECTED PERFORMANCE DEGRADATION CAUSED BY FADING  
MANILA EMBASSY-SANTA RITA DIGITAL LOS LINK

TYPE OF FADING (PREDICTABILITY)	MAGNITUDE (SOURCE)	CORRECTIVE ACTIONS	REMARKS
<b>A. NORMAL</b>			
1. Multipath <sup>1</sup>			
o Flat (95%)	30-35 dB (77 TEP Rpt.)	Use Freq. or Space Diversity	Occurs often.
o Frequency Selective (90%)	3-4 dB (Table 1)	Use Space Diversity and Adaptive Equalization	Measured in TEP tests.
2. Others (90%)	Negligible		Negligible effect from tide height variation Include atmospheric absorption and fog.
<b>B. ABNORMAL</b>			
1. Sub-refractive <sup>2</sup> (50%)	1-3 dB (Figure 11)	Increase path clearance	Occurs seldom. Occurs all year-round.
2. Super-refractive (50%)	7-8 dB (Figure 11)	Use Freq. or Space Diversity	Multi-Fresnel zones.
3. Surface Ducting <sup>1</sup> (5%)	27-37 dB [2]	Use Freq. or Space Diversity	Measured by NAVELEX, worst in April between 1600-1800 hours.
4. Rain Attenuation <sup>1</sup> (50%)	2-10 dB (Figure 14)	Increase Fade Margin	Occurs during May-December.

NOTES: 1. Little multipath or ducting occurs during rain attenuation fading.  
2. Additional losses could be caused by "earth bulge" for inadequate path clearance.

## EMBASSY TO

## SANTA RITA

FREQUENCY IN GHZ =	7.3000E+00
PATH LENGTH IN KILOMETERS =	7.1200E+01
XMTR ANTENNA HEIGHT ABOVE GROUND IN METERS =	2.6000E+01
XMTR HORIZONTAL XMSN LINE LENGTH IN METERS =	8.8000E+00
TOTAL XMTR XMSN LINE LENGTH IN METERS =	3.4800E+01
XMSN LINE TYPE(RECT=1,ELLIP=2,CIRC=3,COAX=4) IS	2
XMSN LINE LOSS FACTOR IN DB/METER =	6.5000E-02
TOTAL XMTR XMSN LINE LOSS IN DB =	2.2620E+00
RCVR ANTENNA HEIGHT ABOVE GROUND IN METERS =	3.4000E+01
RCVR HORIZONTAL XMSN XMSN LINE LENGTH IN METERS =	5.4000E+00
TOTAL RCVR XMSN LINE LENGTH IN METERS =	3.9400E+01
TOTAL RCVR XMSN LINE LOSS IN DB =	2.5610E+00
LCWER RCVR ANTENNA HEIGHT ABOVE GROUND IN METERS =	1.9000E+01
MEDIAN LOS FREE SPACE LOSS IN DB =	1.4682E+02
TOTAL LOSSES(XMTR & UPPER RCVR ANTENNAS) IN DB =	1.5164E+02
TRANSMITTER POWER IN DBM =	3.3000E+01
RECEIVER NOISE FIGURE IN DB =	8.5000E+00
RECEIVER NOISE DENSITY IN DBM/HZ =	-1.6550E+02
MODULATION BIT RATE IN BITS/SEC =	2.6000E+07
REQUIRED EB/NO IN DB FOR BER = 10**-4 IS	2.0000E+01
THRESHOLD FOR FADED RSL IN DBM =	-7.1350E+01
REQUIRED FADE MARGIN IN DB =	3.4672E+01
FADE MARGIN CORRECTION FACTOR IN DB =	4.9000E+00
CORRECTED FADE MARGIN IN DB =	3.9572E+01
TOTAL LINK MARGIN IN DB =	4.5572E+01
TOTAL ANTENNA GAINS(BOTH ENDS) IN DB =	9.2861E+01
CALCULATED ANTENNA DIAMETER IN METERS =	3.4597E+00
ANTENNA DIAMETER CORRECTION FACTOR =	0
PARABOLIC ANTENNA DIAMETER USED IN METERS =	3.66
SINGLE ANTENNA GAIN IN DBI =	4.6056E+01
UNFADED RSL IN DBM =	-2.6527E+01
ACTUAL FADE MARGIN IN DB =	3.8823E+01
AVERAGE YEARLY TEMPERATURE IN DEGREES F =	80.00
YEARLY FRACTION THAT IS FADING SEASON IS	4.0000E-01
TERRAIN ROUGHNESS FACTOR(SMOOTH=6,AVERAGE=15,RCUGH=42) IS	6
CLIMATE FACTOR(HUMID=2,AVG=1,DRY=0.5) IS	2.0
CLIMATE AND TERRAIN FACTOR =	6.5819E+00
DIVERSITY SWITCH FACTOR =	1.7783E+00
RCVR ANTENNA SEPARATION OR EQUIVALENT IN METERS =	1.0000E+01
DIVERSITY FACTOR IS	1.0765E+03
PROBABILITY RSL IS BELOW THRESHOLD PD =	6.7294E-06
Z(MF,D,F) FACTOR =	3.9556E+00
PROB FADE OUTAGE 5 TO 60 SEC =	2.6619E-05

Figure 15. Example of EP 27-77 Link Performance Calculations

diversity configuration using 12 foot antennae 33 feet (10 meter) apart, a total link margin of 45.6 dB summed up from a combination of a fade margin (multipath) of 34.7 dB, a correction factor (atmospheric and rain attenuation) of 4.9 dB, and 6 dB for system miscellaneous losses (refer to calculations of Figure 15 for details). The performance of such a link configuration meets the DCS design criteria for digital LOS links specified in terms of the probability that the fade outage duration will be greater than 5 seconds but less than or equal to 60 seconds and be less than or equal to  $3.69 \times 10^{-5}$  (i.e.  $2 \times 2.6 \times 10^{-7} \times D$ , in km). This is representative of the link performance calculations that account for normal multipath fading, average terrain and climate of the subject link. Other design alternatives satisfying the DCS performance criteria are shown in Table III. Three types of system configurations are compared through power budget trade-offs among various sizes of antenna ranging from 10 to 15 feet, output transmitter power ranging from 2 to 5 watts, and receiver noise ranging from 6 to 10 dB. A retrofit or additional equipment would be required for the parameters listed in Table III that are more stringent than the DRAMA equipment specifications (i.e., 5w power and 6 dB for NF).

TABLE III.

## ALTERNATIVES FOR MANILA EMBASSY-SANTA RITA DIGITAL LOS LINK CONFIGURATION

DIVERSITY (NOTE)	ANTENNA SIZE (FT.)	TRANSMITTER POWER (w)	RECEIVER NOISE FIGURE (dB)
● Dual-Frequency (2F)	15	2	10
	10	5*	10
● Dual-Space (2S)	15	2	10
	12	2	8.5
	10	5*	10
	10	2	6*
● Quad (2F/2S)*	10	2	10

\*DRAMA radio equipment is specified with a xmtr P.O. of 2 w (max), and NF equiv of 8.5 dB (max). Additional equipment, or a retrofit may be required for other values shown for transmitter P.O. (5 w) and NF (6 dB).

NOTE: Improvement factor of 2S is ~ 4 times that of 2F.  
Improvement factor of 2F/2S is slightly better than that of 2S.

#### IV. RECOMMENDED LINK CONFIGURATION

The design alternative recommended for configuration of subject link would provide an optimum link performance through a maximum link margin and an adequate path clearance at the reflection point. This design is constrained by existing antenna tower heights at Santa Rita and possibly a new antenna tower at the Manila Embassy, by ruling-out the addition of an active repeater at Angat, by the parameters specified for DRAMA radio equipment, and expected link performance described above.

Based on the assumptions made throughout this analysis and on the performance degradation summarized in Table II, the following link configuration is recommended:

- (1) Dual space diversity with antenna separation of 33 feet (10 meters). A minimum 120 feet antenna tower height would be required at the Manila Embassy location to accommodate such a configuration.
- (2) Antenna dishes of 12 feet in diameter at each end.
- (3) Transmitter power output of 2 watts.
- (4) If necessary, elevate bore angle of upper antenna at Manila Embassy by  $\approx 0.15^\circ$  to compensate for adverse effects of subrefractive K values (refer to Figure 1 in Appendix A) and to increase penetration angle through an elevated ducting layer (refer to Figure 13). A penalty of  $\approx 1$  dB in signal strength is expected to result from such an offset. Figure 16 shows a typical radiation pattern of a 12 ft. parabolic antenna with a cosine distribution; the arrows point to the  $0.15^\circ$  offsetting in the bore angle and the 1 dB signal degradation. Such an optimization is recommended for implementation based upon results of a performance monitoring activity designed to define ducting/subrefractive adverse conditions.

The performance of the recommended link configuration is expected to meet the DCS performance criteria. Further characterization is recommended to define impact of surface ducting (most severe in April) and subrefractive K variations in terms of signal level attenuation and distribution of occurrences. Route diversity (via Angat and DAU) is recommended for all critical circuits.

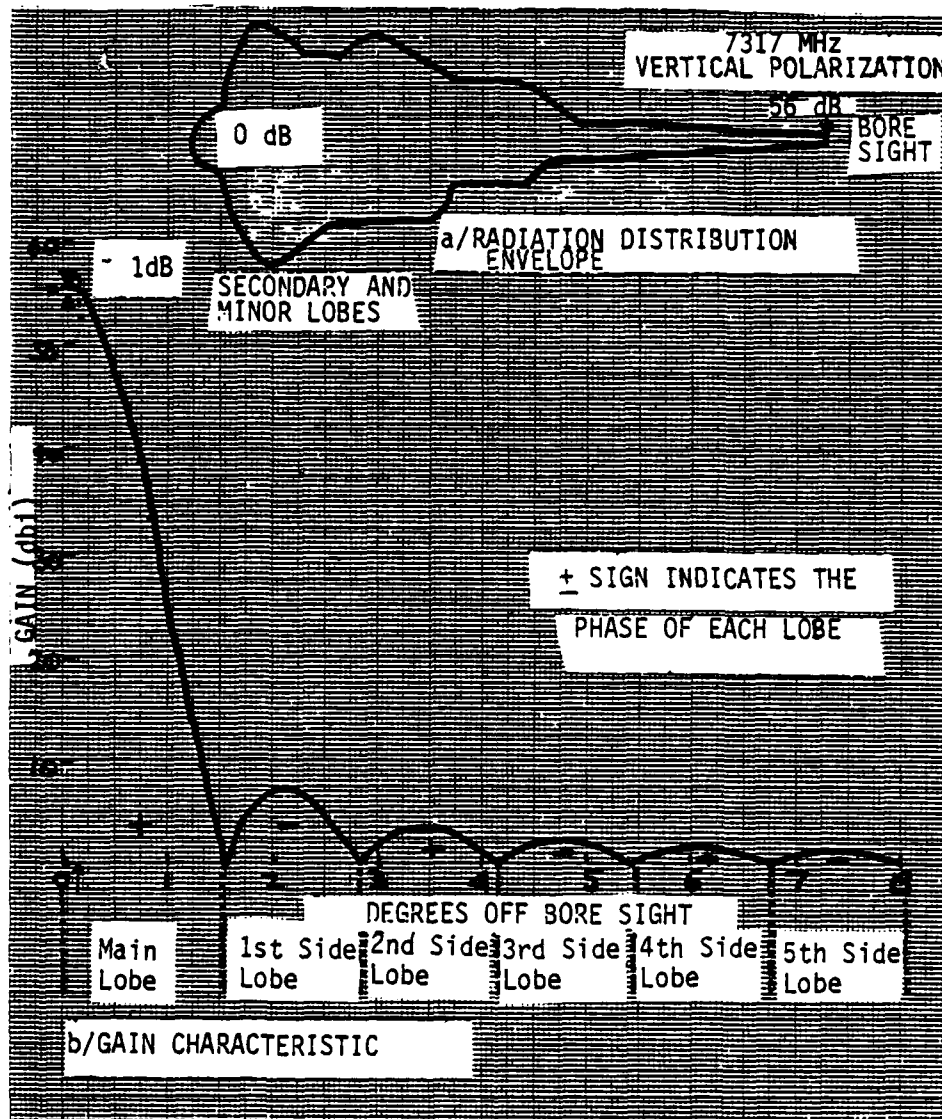


Figure 16. Typical Radiation Pattern of a 12 Ft. Circular Parabolic Antenna



## V. CONCLUSIONS

Various combinations of fading have been identified on the Manila Embassy - Santa Rita radio link which could affect its performance, with the worst offender being a mix of multipath fading and surface ducting conditions prevailing during the dry season months. Partial or total traffic disruption could result from such anomalous propagation conditions.

A digital LOS link configuration in concert with the DCS performance criteria is recommended to alleviate such deleterious effects. This configuration is based on the performance improvement offered by a dual space diversity, availability of the DRAMA radio equipment, a 120-foot antenna tower height at the Manila Embassy location, and if necessary offsetting the antenna bore angle of the upper antenna at the same location.

In addition, based on the link performance degradation expected to be caused mostly by a combination of multipath flat fading and surface ducting, the assessment was made that insignificant improvements would be gained by using the DRAMA radio equipment in a quadruple or hybrid diversity configuration, or by using a non-DRAMA radio equipment with an adaptive equalizer.

#### REFERENCES

- [1] OT Report 75-59, "Refractivity Gradients in the Northern Hemisphere," Sampson, C. A. (1975).
- [2] US NAVELEX Research Report 566, "Propagation Characteristics of a Proposed Microwave Communication System in the Philippine Islands," Hopkins, R. U. F., and Hughes, L. R. (1975).
- [3] GTE Lenkurt Inc., Engineering Considerations for Microwave Communications Systems, Engineering Report, (1975).
- [4] USNSEEAC Philippines (1980), Philippine DCS Digital Microwave, U.S. Embassy, Preliminary BESEP.

## APPENDIX A

DETERMINING THE K FACTOR TO USE IN LOS  
MICROWAVE LINKS FROM CUMULATIVE PROBABILITY  
DISTRIBUTIONS OF THE REFRACTIVITY GRADIENT DATA,  
 $dn/dh$ , FOR A GIVEN K FACTOR AVAILABILITY

## BACKGROUND

In many parts of the world, there are frequent occasions where the K factor, effective earth radius, is less than unity. This condition is frequently referred to as inverse bending and is caused by a subrefractive atmosphere. The effect produced is that of the earth bulging up into the microwave path which starts to block the path (no longer LOS); the diffraction mode of propagation then comes into play causing increased path loss. This loss of signal due to inverse bending is usually counteracted by providing more path clearance.

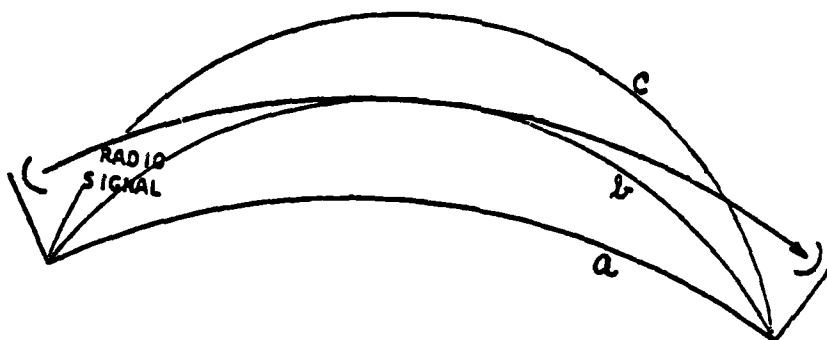
## PURPOSE

The purpose of this paper is to present a technique which would be applicable to determining the K value to be used in LOS microwave path engineering when a value of media availability is to be met on a LOS path in a particular region of the world.

## TECHNICAL DISCUSSION

Substandard or less than standard refraction occurs with certain meteorological conditions which causes the atmospheric density to actually increase with height. This condition described earlier as earth's buldge or inverse beam bending, causes an effective upward curvature of the earth as shown in Figure 1. A substandard atmospheric condition may occur through the formation of fog created with the passage of warm air over cool air or a moist surface. This will cause the atmospheric density to be lower near the ground than at higher elevations, causing an upward bending of the beam. Fog is simply a form of stratus cloud lying very close to the ground. One type, known as a radiation fog, commonly accompanies temperature inversion and is formed at night when temperature of the basal air falls below the dew point. Another type, advection fog, results from the movement of warm, moist air over a cold or snow-covered ground surface. Losing heat to the ground, the air layer undergoes a drop of temperature below the dew point, and condensation sets in. A similar type of advection fog is formed over oceans when a warm current blows across the cold surface of an adjacent cold current. Fogs of the Grand Banks off Newfoundland are largely of this origin because here the cold Labrador current comes in contact with warm waters of the Gulf Stream. Coastal areas and river valleys are especially likely to have anomalous propagation (substandard) relative to air stratification, and extreme refractivity values are most likely to occur in layers of rather limited vertical extent. Tropical and sub-tropical regions generally have larger diurnal and interdiurnal variations in refractivity gradients than do temperate regions. Refractivity is highly sensitive to humidity. Figure 2 illustrates the Koppen-Geiger climate system of the world which is useful in predicting where in the world these substandard regions occur.

Collins Radio<sup>(2)</sup> has treated the effect of earth (bulge) clearance on the free space path loss, as outlined here. Figure 3, taken from Bullington's article on Radio Propagation, BSTJ, May, 1957, shows the effect of clearance on the transmission loss relative to free space. The terms used in Figure 3 are as follows:



- a. Normal refractivity condition.
- b. Grazing refractivity condition.
- c. Earth bulge refractivity condition,  
diffraction mode. ( $K$  could be  $2/3$  and lower).

Figure 1. Simplified Diagram Illustrating Inverse Bending

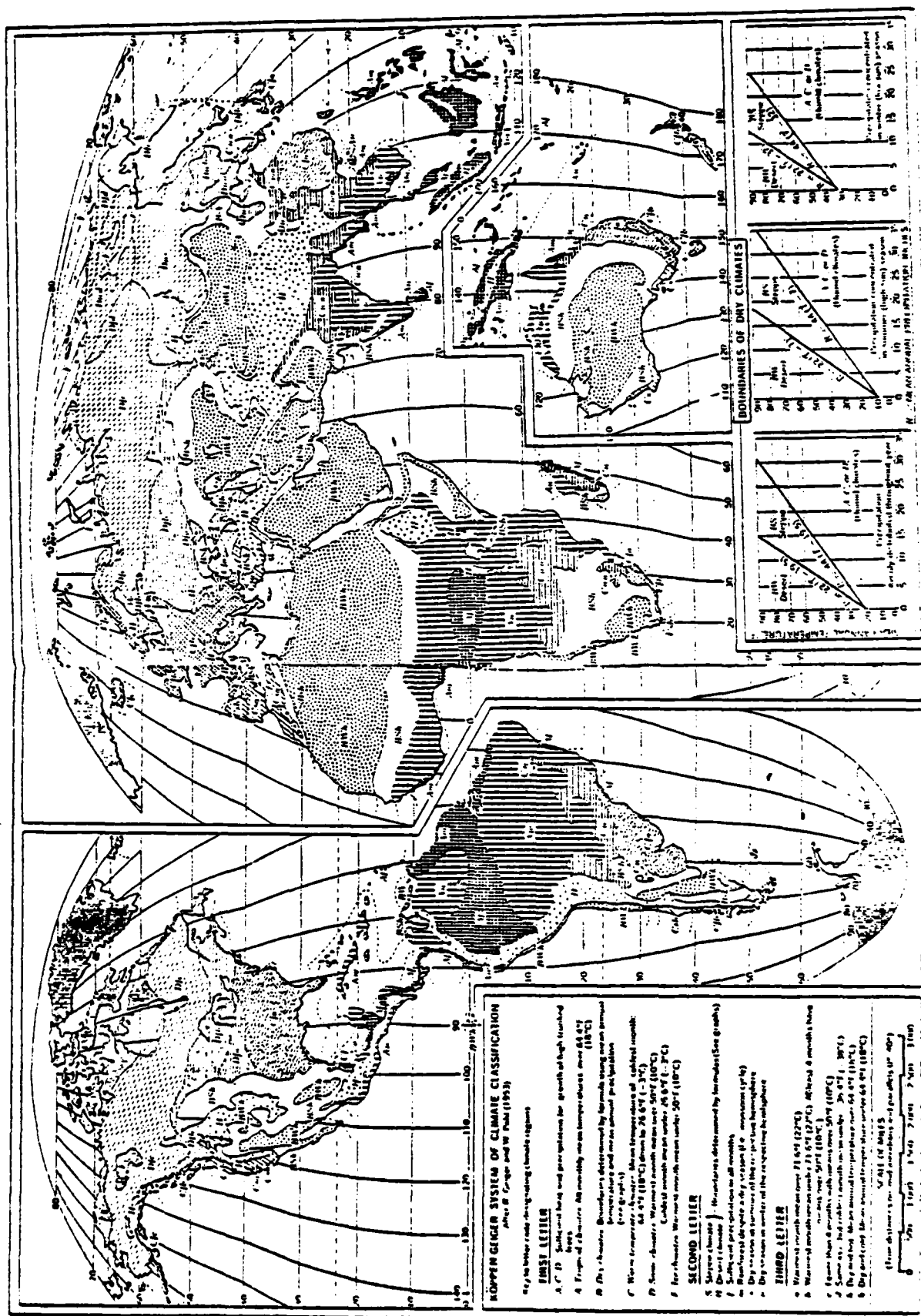


Figure 2. World Map of Köppen - Geiger Climate System from (1)

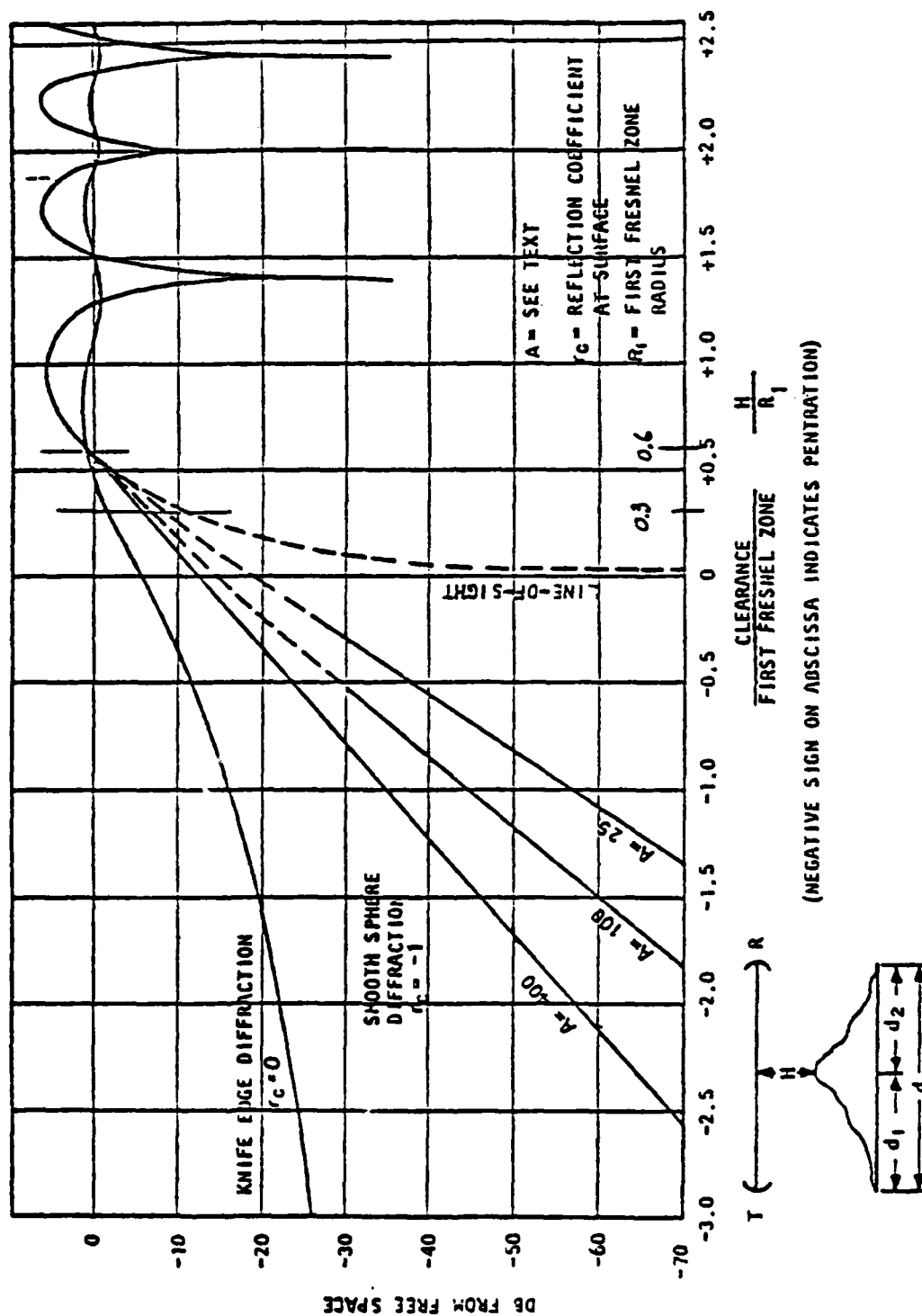


Figure 3. Effect of Clearance on Radio Transmission

$$A = \frac{h_1}{\sqrt[3]{k}} \left[ \frac{\left(1 + \sqrt{\frac{h_2}{h_1}}\right)^2}{2} \right] \left[ \frac{F}{4000} \right]^{\frac{2}{3}} \quad (1)$$

$h_1$  and  $h_2$  = absolute antenna heights, ft.

$K$  =  $\frac{\text{effective earth radius}}{\text{true earth radius}}$

$F$  = operating frequency, MHz

$r_c$  = reflection coefficient of surface

( $r_c = -1$  smooth sphere diffraction)

$H$  = clearance, ft.

$R_1$  = first Fresnel radius, ft.

The attenuation due to inverse bending may be estimated assuming different values of  $K$ . Earth bulge may be calculated as:

$$h = 0.667 d_1 d_2, \quad (2)$$

resulting in the earth bulge,  $h$ , assuming a  $K$  factor of unity (true earth radius). It may be expressed in more general terms as

$$\text{Earth bulge, } h = 0.667 \frac{d_1 d_2}{K} \quad (3)$$

where,

$h$  = earth bulge, feet

$d_1$  = distance from initial end of system, miles

$d_2$  = distance from far end of system, miles

$K = \frac{\text{effective earth radius}}{\text{true earth radius}}$

A path would normally be designed to allow at least 0.3 fresnel zone clearance. In areas where the  $K$  factor is subject to severe variation, the earth bulge can be estimated for the lowest  $K$  factor. From this,



the amount of reduced clearance can be estimated. Then, using Figure 3, the magnitude of the fade can be estimated assuming smooth sphere diffraction.

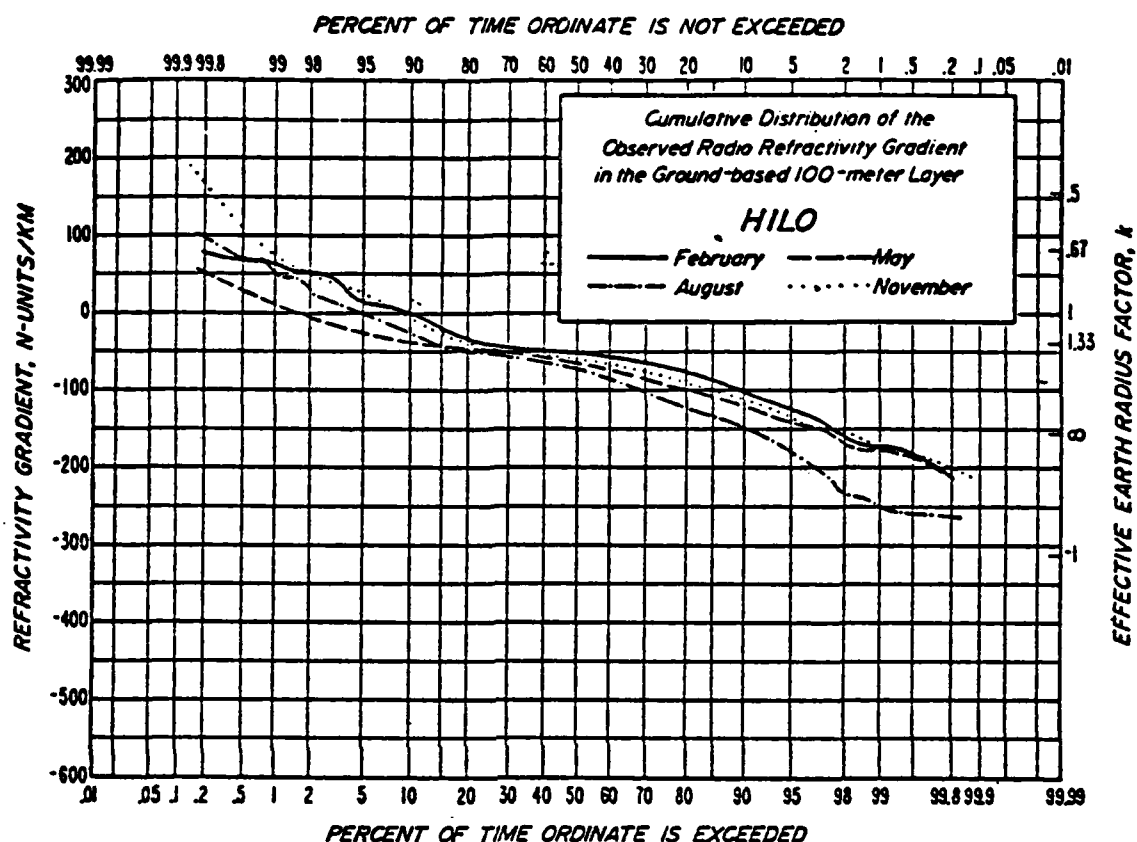
Basically, the problem of fading due to inverse bending is combated by providing larger Fresnel radius clearance. It is sometimes more economical to provide additional fade margin in the form of a larger antenna and higher power transmitters.

#### DETERMINING K FACTOR FOR A REGION

The data needed to determine the K factor for a given region is the cumulative refractivity gradients for the region of concern. Information on the refractivity gradients to be expected in any part of the world is available in several publications.(3, 4, 5) These data are the best available at the present time and they have some serious shortcomings. These will be explained in the following paragraphs. These references contain maps showing the 100-m gradients exceeded for selected percentages of time. For application to the design of radio links, many engineers prefer a complete cumulative time probability distribution of the gradients at specific locations. Data for 4 months of the year are shown on the same graph to facilitate seasonal comparisons. Accompanying each graph is information on the length of record analyzed, the hours at which observations were taken, and general climatic and topographic details in the vicinity of the station. Figure 4 is data for Hilo, Hawaii from reference (5) and is typical of the data available. This data will be used in this report for illustrative purposes.

Refractivity gradients can be calculated from the radiosonde observations (RAOBs) made by national meteorological services in the various countries. However, these observations of the vertical changes in temperature, pressure, and humidity do not provide as much detail and accuracy as is desirable for studies of radio refractivity.

Climatological RAOB data for the United States and many foreign locations are on file at the National Climatic Center in Asheville, N.C. The analysis of these data to obtain refractivity statistics requires that the refractive index be calculated for the individual data points on each sounding; an interpolation must be made to obtain the refractivity value at the desired height, and the gradient over the interval can then be calculated. To avoid possible misleading indications related to the year-to-year variations in weather conditions, data for a number of years must be considered if a good climatological average is to be obtained. Climatic data for a 5-year period, including two observations per day, were used in this analysis. Only one month in each season was processed, and the observations at different times of day were not treated separately. Stations were selected to provide wide geographical coverage, rather than to give a dense coverage in a few areas. Each graph in reference (5) has a dual scale on the ordinate to show both the refractivity gradient in N-units/km and the equivalent effective earth radius factor, "K", which is used to compensate for ray bending in terrain profile



### Hilo, Hawaii

19-44 N, 155-04 W.

11 meters MSL

Data: Radiosonde.

0300 and 1500Z (1700 and 0500 LST)

8/52 - 8/54 and 2/55 - 5/57

(Also 0300, 0900, 1500, and 2100Z for 11/54 only)

Temperature (°F):

January 79/63; July 82/67

Mean Dewpoint (°F):

January 62; July 68

Precipitation (inches):

Annual 136.6; December 15.18; June 6.79

Station is located near the eastern shore of a large, mountainous island (area 4038 sq. miles; peaks above 13600 ft); it is within the northeast trade wind belt. Day-to-day and seasonal weather changes generally small at locations near sea level, but temperatures, precipitation, and cloudiness in vicinity vary greatly with elevation and degree of exposure to the trade winds.

Figure 4. Cumulative Refractivity Gradient for Hilo, Hawaii

analysis of radio links. The factor "K" is related to the refractivity gradient  $N/h$  in N-units/km by

$$k = \left[ 1 + 6370 \frac{\Delta N}{\Delta h} \times 10^{-6} \right]^{-1} \quad (4)$$

where 6370 km represents the actual earth radius.

Also:

$$k = \frac{1}{\left[ 1 + \frac{dN}{dh} \right]} \quad (5)$$

The graphs show the cumulative distribution of the radio refractivity gradients in the ground-based 100-m layer, as calculated from an radiosonde observations during the period specified under "Data".

Figure 4 shows the percentage of the observations in which various refractivity gradients were found in the lowest 100 meters; they do not indicate the percentage of time in a year that such gradients can be expected. Although the latter statistics are desired for propagation and system performance estimates, the available data are insufficient to make such a determination. The radiosonde package rises through the lowest 100-m layer in less than 30 seconds, and this only twice a day at most stations. Thus, we have available two very brief samplings of atmospheric structure daily, rather than frequent or continuous measurements. It seems unlikely that the extremes of the diurnal gradient variation would always occur at 0000Z and 1200Z (or 0300Z and 1500Z); therefore the refractivity gradient statistics based on RAOBs can be assumed to show a lower probability of occurrence of the extreme gradients than would be the case if observations were made hourly.

The graphs in the references are especially useful for station-to-station comparisons, such as estimating the probability of subrefraction in two areas with differing climates where performance data are available for only one of the areas. Thus, the relative probability of a certain K-value being exceeded can be estimated by reference to the graphs, as can strong superrefraction or ducting. In making such estimate, however, one should check both the length of record and the number of observations per day at a particular station. Also, the local time of the observations should be considered; for example, a distribution based primarily on nighttime (or only daytime) observations may give a distorted indication of the overall probability of occurrence of various gradients.

Variations in refractivity gradients tend to be closely related to the local or sun-referenced time, because of the influence of heating and cooling of the earth's surface on the stratification of air layers near the ground. For example, extreme gradients of refractivity often occur near sunrise when nocturnal temperature inversions tend to be most pronounced, and near sunset when there is a rapid shift from gain to loss of heat in the air layer near the ground. RAOBs, however, are taken at standard times which do not always coincide with the local time when extreme gradients are most likely to occur. The variation of sunrise/sunset times during the year should also be considered, particularly at high-latitude stations. The atmospheric layers near the surface are greatly influenced by terrain features, ground moisture sources, and vegetation; thus, on most long overland paths, low-level refractivity gradients can be expected to vary by appreciable amounts over distances on the order of a few kilometers. The net result of this variation in space should be to produce less extreme effective path gradients than might be assumed from consideration of radiosonde data at one point on the path. On the other hand, the RAOB data are likely to yield conservative indications of gradient intensity because of the very limited sampling periods per day. This poses a dilemma not easily resolved. The relationship between point and path refractivity is not known, and the total time per year in which certain gradients will affect a given path must be estimated from the statistics of occurrence during two very brief observations each day at some weather station possibly hundreds of kilometers from the radio path.

The more extreme positive refractivity gradients near the surface are greatly influenced by local conditions of terrain, moisture sources, etc., and are not likely to extend over wide areas. A further comment from Lenkurt(6), is as follows:

"Experience has indicated that, for actual microwave paths, the effective  $k$  over the entire path reaches a very high or very low value for a much smaller percentage of time than would be indicated by the distribution of  $k$  values as found by meteorological measurements at single points. The most probable explanation is that the usual conditions causing these extreme values are unlikely to occur over more than a small part of the path of any given instant."

Coastal areas and river valleys are especially likely to have anomalous propagation related to air stratification, and extreme refractivity values are most likely to occur in layers of rather limited vertical extent.

Tropical and subtropical regions generally have larger diurnal and interdiurnal variations in refractivity gradients than do temperate regions. Extreme gradients are also much more common in the tropics, and over layers of limited thickness (up to a few tens of meters) may at times exceed +1000 N-units/km. Use of the data from the nearest RAOB station is not always a satisfactory approach to radio-climatological estimates in the tropics, unless local modifications of the indicated refractivity are considered.

The refractivity is highly sensitive to humidity, which can change rapidly over comparatively limited horizontal or vertical distances in the tropics. Such changes often occur in land/sea breeze circulations, trade-wind subsidence regions, and monsoonal flows. At higher latitudes, however, the movement of air masses involved in large-scale weather systems may effectively produce a temporary "tropical" environment in a normally "temperate" region, as when warm, moist air masses move over the central United States from the Gulf of Mexico. Thus the extreme gradients common to many tropical regions can also be expected to occur at times in more temperate regions.

In summary, the available data on refractivity gradients is deficient for use by engineers to perform detailed K factor analysis on microwave paths in the following areas:

1. Few number of point observations per day.
2. Only one month of data in each 3 month season was processed.
3. Observations at different times of day were not treated separately.
4. Stations selected to give geographical coverage, rather than dense coverage in a few areas.
5. Some data are based on only one month of observations.
6. The time of day most data are taken does not correspond to the local time when extreme gradients are most likely to occur.

Notwithstanding the above discussion, the following procedure can be used to determine "ball park" values of K factors for problem regions. Once more accurate and fine grain data is provided on cumulative refractivity gradients, more accurate values of K factors can be calculated by using the following techniques.

#### K FACTOR DETERMINATION PROCEDURE

Figure 4 will be used to determine the K factor to be used in LOS path engineering analyses for the region of Hilo, Hawaii. The problem is to determine a K factor for the area so that this K value is not exceeded for a certain K factor availability, in percent of a year. Let us use, as an example, 99.9% of the year for the K factor availability.

Notice in looking at Figure 4 that data are scarce for large values of positive refractivity gradient area of the graph. The only recourse for this analysis, keeping in mind the limitations of this chart as discussed in previous section, is to extrapolate into the uncharted region of the graph. This has to be done with extreme caution. This can be done by observing the trend of the curves in the rest of the graph. Figure 5 is such an extrapolated graph from Figure 4 and shows the relationship of refractivity to percent of time in the higher availability areas.

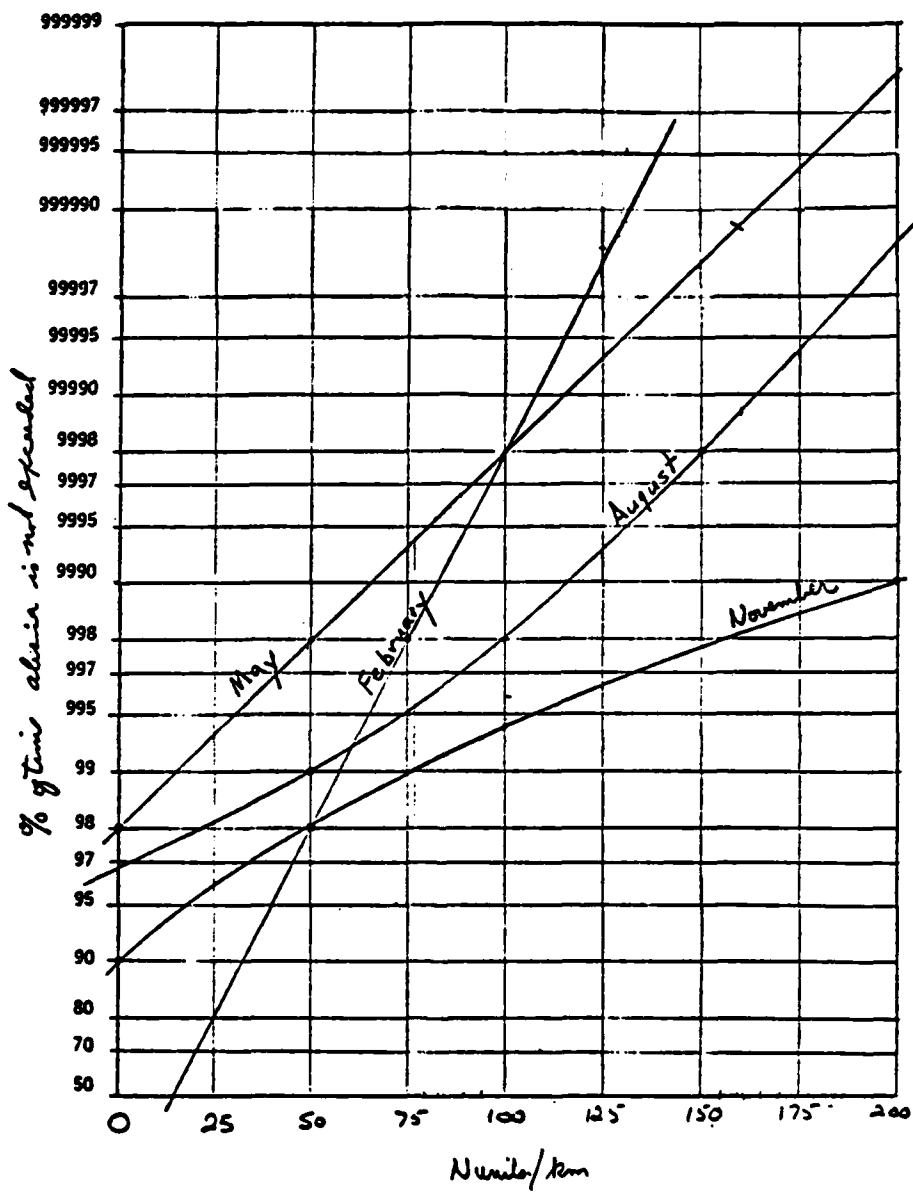


Figure 5. Cumulative Refractivity Gradient Extrapolated for Higher Time Availability

The next step is to prepare a table as shown in Table 1 in which data from Figure 5 are entered for several K factors (and refractivity gradients) and for the 4 months of the year, as shown in Figure 4. There are 2191.5 hours in a typical 3 month period and 8766 hours in a year. Since each of the months in Figure 4 represents really 3 months of data, the percentage of time the K factor is exceeded is multiplied by the number of hours in 3 months and this represents the number of hours that particular gradient is exceeded during that period. This number of hours is entered in the appropriate place in Table 1. Once this is accomplished for all gradient values of interest, the sum of the hours is taken for each gradient value and this sum is then the number of hours in the year that this gradient value is exceeded. To determine the media availability for the year, divide into this year sum hours the total number of hours in a year (8766 hr) and subtract this q from one, which gives the yearly value of refractivity gradient (or K factor) which is not exceeded for each of the K factors (last column in Table 1). These K values are then plotted on probability paper as shown in Figure 6. From Figure 6, it is seen that a K factor availability of 0.999 is obtained when using a K factor of approximately 0.5 in the Hilo, Hawaii region.

The actual value of K factor is more than likely larger than this, but due to the coarse grain of the available data, the distribution of the refractivity gradient during any 3 month period is not known, and these data are needed if more accurate K factors are to be determined. The procedure outlined above still holds; just more accurate data is needed.

The determination of media availability from the K factor availability will be discussed in a future paper. This has to do with determining the distribution of increase of free space path loss as a function of the prevailing K factor in a certain region by the implementation of Figure 3 in this report.

TABLE 1. CALCULATION PROCEDURE

K FACTOR	N-UNIT/ km	FEB		MAY		AUG		NOV			
		1	2	1	2	1	2	1	2	3	4
0.76	50	0.980	43.83	0.998	4.38	0.99	21.92	0.98	43.83	131.49	0.9850
0.67	78.5	0.9992	1.75	0.99955	1.0	0.996	8.77	0.992	17.53	29.05	0.99668
0.61	100	0.9998	0.44	0.9998	0.44	.998	4.38	.994	13.15	18.41	0.99790
0.56	125	0.999978	0.05	0.99993	0.15	.99935	1.42	.9963	8.11	9.73	0.99889
0.5	157	0.999999	0.01	.999985	0.033	.99987	0.28	.9965	7.67	7.99	0.99909
0.47	175	0.999999	0.01	.999994	0.01	.99994	0.13	.9984	3.51	3.66	0.9995825
0.44	200	0.999999	0.01	.999998	0.01	.99998	0.04	.999	2.19	2.25	0.99974
0.28	400	0.999999	0.01	.999999	0.01	.999999	0.01	.99994	0.13	0.16	0.999982

- h. JFS:
1. K factor availability for the 3 month period.
  2. Number of hours the k factor is not exceeded for the 3 month period.
  3. Number of hours the k factor is not exceeded for the year.
  4. K factor availability for the year.



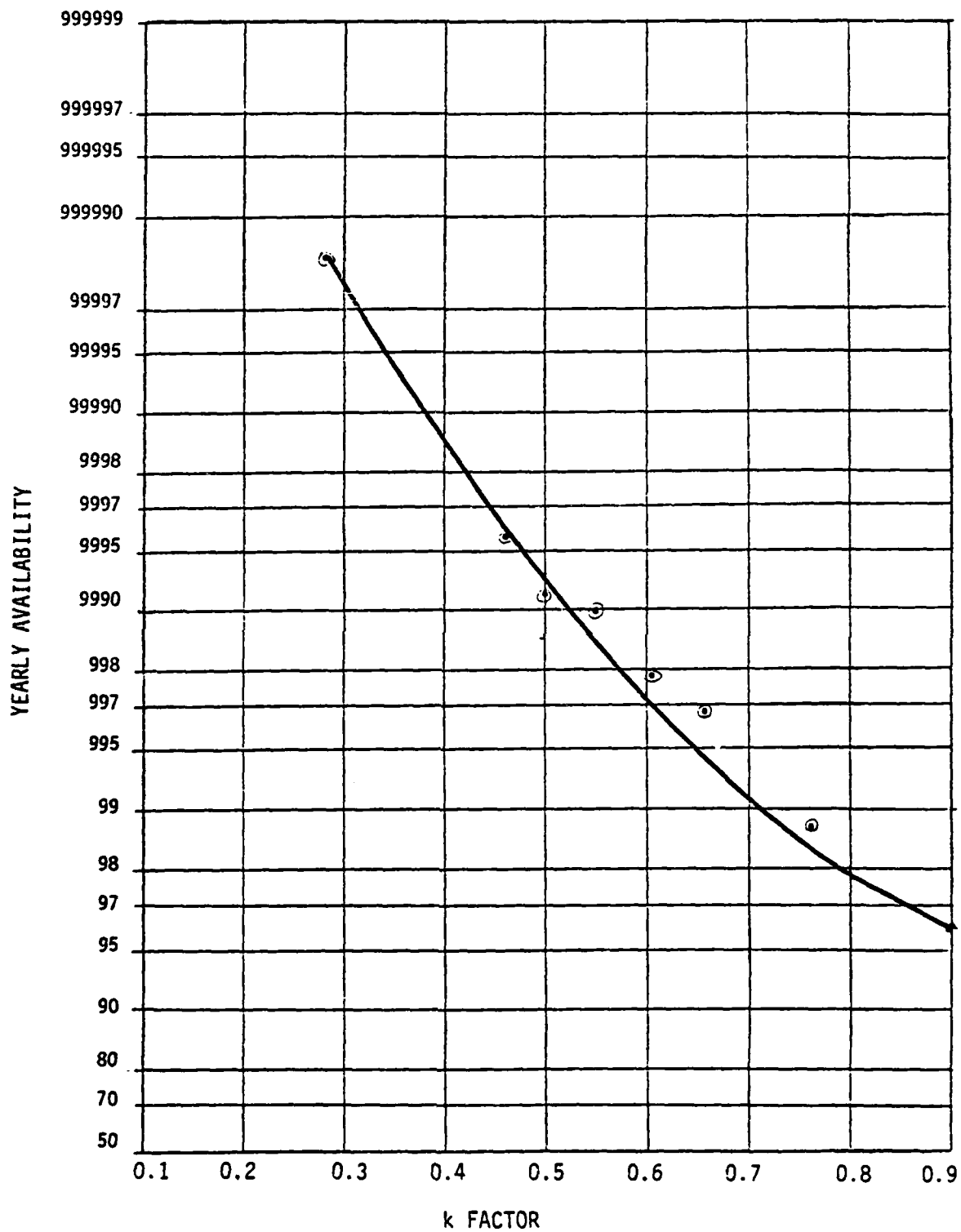


Figure 6. Yearly Availability of K Factor

## REFERENCES

1. Strahler, A. N., Physical Geography, Second Edition, John Wiley & Son, Inc., New York, 1959.
2. Collins Radio Company, "Propagation Considerations for 6 and 12 GHz Microwave Communication Systems", CEL-22, September 10, 1962.
3. Bean, B. R., B. A. Cahoon, C. A. Samson, and G. D. Thayer (1966), "A World Atlas of Atmospheric Radio Refractivity", ESSA Monograph 1 (NTIS, AD648805).
4. NBS Monograph 22, "Climatic Charts and Data of the Radio Refractive Index for the United States and the World", 1960.
5. OT Report 75-59, Samson, C. A., "Refractivity Gradients in the Northern Hemisphere", April 1975.
6. Lenkurt 6000 MC-ENG-1, "Microwave Path Engineering Considerations 6000-8000 MHz", September 1961.

APPENDIX B

FADING CHARACTERISTICS FOR OVER-THE-WATER  
MICROWAVE LINKS

## APPENDIX B. FADING CHARACTERISTICS FOR OVER-THE-WATER MICROWAVE LINKS

In this appendix, a mathematical model for predicting the characteristics of a received microwave signal modified by interference due to reflections from the sea is described. The change in absolute signal level or fading depth depends on the state of polarization of the radiation, the characteristics of the sea and the geometry of the radio link. The geometry which defines the relative positions of the transmitter, receiver and reflection zone allows for earth curvature. Plane polarized radiation is assumed with circular aperture using parabolic antennas. Also, an allowed seafloor variation is built into the model.

After presentation of this model, the Santa Rita - Embassy link analysis is set up by showing values selected for input to the model. Finally, the computer program written for this model is attached.

### 1. Flat Earth Geometry

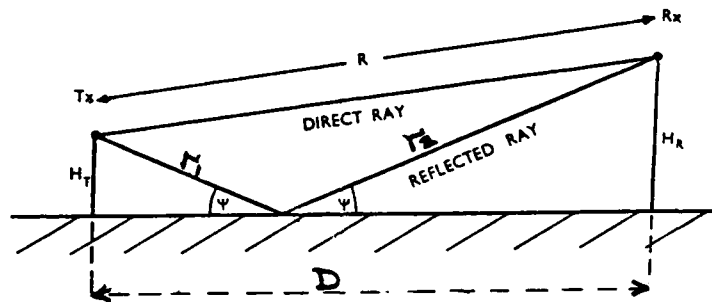


Figure 1. Flat Earth Geometry

a. Grazing Angle. From the geometry in Figure 1 it is clear that the angle of incidence and hence the angle of reflection  $\psi$  is given by:

$$\tan \psi = \left( \frac{H_T + H_R}{D} \right) \quad (B.1)$$

where

$H_T$  = transmitter height above MSL - sea tide height  
 $H_R$  = receiver height above MSL - sea tide height  
 $D$  = Path length.

b. Path Difference. Also from the geometry in Figure 1, the direct ray has length

$$R = \sqrt{(H_R - H_T)^2 + D^2} \quad (B.2)$$

and the reflected ray has length

$$r_1 + r_2 = \frac{H_T}{\sin \psi} + \frac{H_R}{\sin \psi} \quad (B.3)$$

The path difference is therefore

$$\Delta R = (r_1 + r_2) - R \quad (B.4)$$

## 2. Correction For Curved Earth

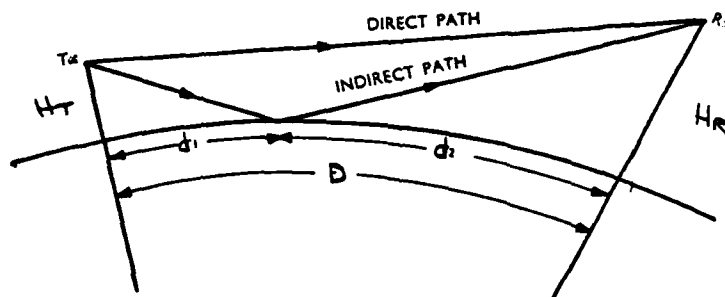


Figure 2. Curved Earth Geometry

Figure 2 illustrates the pertinent geometry for curved earth. From reference 1, it is shown that

$$d_2 = \frac{D}{2} + P \cos \left( \frac{\phi + \pi}{3} \right) \quad (\text{B.5})$$

where

$$P = \frac{2}{\sqrt{3}} \sqrt{a_e (H_T + H_R) + (D/2)^2} \quad (\text{B.6})$$

and

$$\phi = \cos^{-1} \left[ \frac{2a_e (H_R - H_T) D}{P^3} \right] \quad (\text{B.7})$$

and  $a_e$  = earth radius (3958.32 miles).

We now define four parameters,  $S$ ,  $S_T$ ,  $S_R$ , and  $T$ :

$$S_T = \frac{d_1}{\sqrt{2a_e H_T}} \quad (\text{B.8})$$

$$S_R = \frac{d_2}{\sqrt{2a_e H_R}} \quad (\text{B.9})$$

$$S = \frac{D}{\sqrt{2a_e H_T} + \sqrt{2a_e H_R}} \quad (\text{B.10})$$

$$T = \sqrt{\frac{H_T}{H_R}} \quad (\text{B.11})$$

The three correction factors for curved earth are then defined in terms of these four parameters

$$D(S, T) = \left( 1 + \frac{4S_T^2 S_R T}{S(1-S^2)(1+T)} \right)^{-1/2} \quad (\text{B.12})$$

$$J(S,T) = (1 - S_T^2)(1 - S_R^2) \quad (B.13)$$

$$K(S,T) = \frac{(1 - S_T^2) + T^2(1 - S_R^2)}{1 + T^2} \quad (B.14)$$

a. Grazing Angle. The grazing angle corrected for curved earth is given by

$$\tan \psi_c = \frac{H_T + H_R}{D} \cdot K(S,T) \quad (B.15)$$

b. Path Difference. The path difference corrected for curved earth is given by

$$\Delta R_c = [(r_1 + r_2) - R] \cdot J(S,T) \quad (B.16)$$

### 3. Ratio of Resultant Signal to Direct Signal

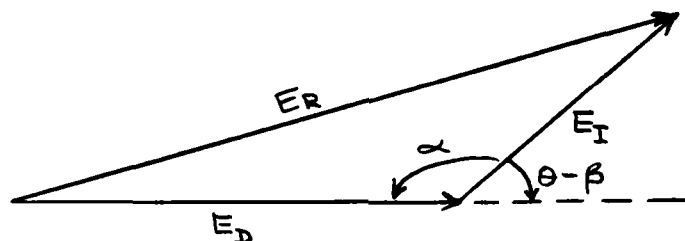


Figure 3. Two Ray Geometry

Consider a two path microwave link with

$E_R$  = amplitude of resultant

$E_D$  = amplitude of direct path

$E_I$  = amplitude of indirect (reflected) path.

By the simple geometry of Figure 3 and the law of cosines

$$E_R^2 = E_D^2 + E_I^2 - 2 E_D E_I \cos(\theta - \beta) \quad (B.17)$$

Defining  $\alpha = 180^\circ - (\theta - \beta)$  , the above expression becomes

$$E_R^2 = E_D^2 + E_I^2 + 2E_DE_I \cos(\theta - \beta) \quad (B.18)$$

or

$$E_R/E_D = \sqrt{1 + m^2 + 2m \cos \gamma} \quad (B.19)$$

where

$$m = \frac{E_I}{E_D} = \text{degradation of the indirect signal in relation to direct signal}$$

$$\gamma = \theta - \beta = \text{phase difference between direct and indirect signals}$$

$$\beta = \text{phase shift due to reflection off surface of earth}$$

$$\theta = \text{physical path length difference expressed in radians.}$$

The ratio,  $m$  , of indirect to direct signals is a function of the antenna radiation pattern, the magnitude of the reflection coefficient, and the divergence factor, as shown below:

$$m = D_c R_v E_T E_R \quad (B.20)$$

where

$D_c$  = divergence factor,  $D(S,T)$ , for curved earth

$R_v$  = magnitude of the reflection coefficient

$E_T$  = ratio of signal at boresight of transmit antenna to signal off boresight in direction of reflection point on surface of earth

$E_R$  = same as  $E_T$  but for receive antenna.



Also, taking into account the antenna geometry

$$\gamma = \theta - \beta - \epsilon_T - \epsilon_R \quad (B.21)$$

where  $\theta$  and  $\beta$  are as previously defined and

$\epsilon_T, \epsilon_R$  = are 0 when reflected signal is in main lobe of antenna pattern or in an even numbered side lobe, and are  $\pi$  radians when reflected signal either enters or leaves an odd numbered side lobe of the antenna.

a. Calculation of Divergence Factor. Radiation reflected from a spherical surface diverges at a greater rate after reflection than it would from a plane surface. To allow for this, the divergence factor  $D(S,T)$  is introduced. This factor modifies the reflection coefficient as a multiplying factor in the same way as the grazing angle and path difference were modified. See Eq. (B. 12).

b. Calculation of Complex Reflection Coefficient. For vertically polarized radiation the complex reflection coefficient is [2]:

$$R_V e^{j\beta_V} = \frac{Z \sin \psi_c - \sqrt{Z - \cos^2 \psi_c}}{Z \sin \psi_c + \sqrt{Z - \cos^2 \psi_c}} \quad (B.22)$$

and for horizontally polarized radiation

$$R_H e^{j\beta_H} = \frac{\sin \psi_c - \sqrt{Z - \cos^2 \psi_c}}{\sin \psi_c + \sqrt{Z - \cos^2 \psi_c}} \quad (B.23)$$

where

$R_{V,H}$  represents amplitude change due to reflection for vertical and horizontal polarization

$\beta_{V,H}$  represents phase change due to reflection for vertical and horizontal polarization

and

$$Z = \epsilon_r - j \left( \frac{18000 \sigma}{f} \right) \quad (B.24)$$

where

$\epsilon_r$  = relative permittivity of the medium

$\sigma$  = conductivity, mho-meters/square meter

$f$  = carrier frequency in MHz.

c. Calculation of Antenna Patterns

The relation between the field strengths of direct versus reflected paths may be expressed conveniently as a ratio. From Figure 4, this ratio for the transmit antenna is given by

$$E_T = \frac{E_{RT}}{E_{OT}} \quad (B.25)$$

and for the receive antenna is given by

$$E_R = \frac{E_{RR}}{E_{OR}} \quad (B.26)$$

For parabolic antennas (circular aperture) the field intensity is proportional to [3]:

$$E(\eta) = \frac{2\pi r_o^2 J_1(\alpha)}{\alpha} \quad (B.27)$$

where

$$\alpha = \frac{2\pi r_o}{\lambda} \sin \eta$$

$J_1(\alpha)$  = first-order Bessel function

$r_o$  = antenna radius

$\eta$  = angle of antenna with respect to boresight.

Using the geometry of Figure 4, we can calculate the antenna angles off boresight toward the reflection point. For the flat earth model,

$$\eta_T = \psi_f + \tan^{-1} \left( \frac{H_R - H_T}{D} \right) \quad (B.28)$$

$$\eta_R = \psi_f - \tan^{-1} \left( \frac{H_R - H_T}{D} \right) \quad (B.29)$$

For curved earth, the above two expressions are modified by  $K(S,T)$  as follows:

$$\eta_{TC} = \tan^{-1} \left[ K(S,T) \cdot \tan \eta_T \right] \quad (B.30)$$

$$\eta_{RC} = \tan^{-1} \left[ K(S,T) \cdot \tan \eta_R \right] \quad (B.31)$$

The four field strengths,  $E_{RT}$ ,  $E_{OT}$ ,  $E_{RR}$  and  $E_{OR}$ , may be calculated using Eq. (B. 27) in conjunction with Eqs. (B. 30) and (B. 31).

4. Application to Phillipines Link. Table I shows pertinent link parameters for the Manila Embassy - Santa Rita link. Finally, a listing of the computer program with subroutines is included, which was used to obtain results shown in the main body of this report.

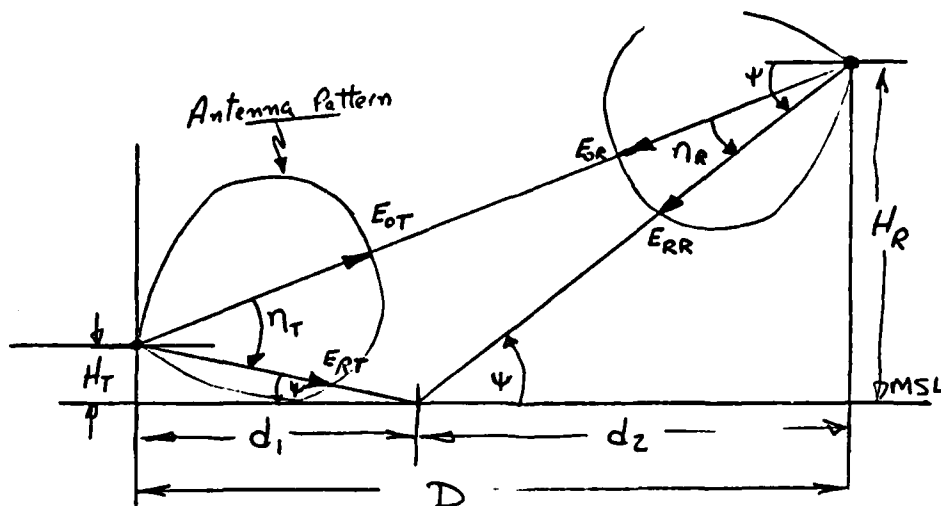


Figure 4. Antenna Pattern Geometry

TABLE I  
MANILA EMBASSY - SANTA RITA LINK PARAMETERS

Frequency: 7317 MHz

Site Evaluation: Embassy = 8 feet  
Santa Rita = 1550 feet

Antenna Height ( $H_T$ ,  $H_R$ ): Embassy = 85 feet  
Santa Rita = 110 feet

Path length (D): 44.12 miles

Tide Variations: -1.0 feet to +4.0 feet

Relative permittivity of the Reflection Surface ( $\epsilon$ ): 81

Conductivity of reflection surface ( $\sigma$ ): 4.64

Antenna diameter ( $2r_0$ ): 12 feet

#### REFERENCES

1. D. E. Kerr, "Propagation of Short Radio Waves", M.I.T. Radiation Laboratory Series, Vol. 13.
2. Henry R. Reed and Carl M. Russell, Ultra High Frequency Propagation, Science Paperbacks and Chapman & Hall Ltd, 1966.
3. Merrill J. Skolnik, Introduction to Radar Systems, McGraw-Hill Book Company, Inc., 1962.
4. D. R. Gager, "Signal Fading Characteristics Due to Reflections from the Sea", The Marconi Review, Vol. XXXIV, No. 180, 1971.

UNCLASSIFIED

TRANSMITTER SITE	EMBASSY	RECEIVER SITE	SANTA RITA	FREQUENCY (MHZ)	7317.00	PATH LENGTH (MI)	49.12	TRANSMITTER SITE ELEVATION ABOVE MSL (FT)	8.00	TRANSMITTER ANTENNA HEIGHT ABOVE GROUND (FT)	85.00	RECEIVER SITE ELEVATION ABOVE MSL (FT)	1550.00	RECEIVER ANTENNA HEIGHT ABOVE GROUND (FT)	110.00	EFFECTIVE EARTH RADIUS FACTOR	0.67	ACTUAL EARTH DIAMETER (MI)	3958.32	MAX HIGH TIDE ABOVE MSL (FT)	4.00	MAX LOW TIDE BELOW MSL (FT)	-1.00	TIDE INCREMENT (FT)	1.00	RECEIVED MINIMUM HEIGHT (FT)	1550.00	RECEIVED HEIGHT INCREMENT (FT)	10.00	POLARIZATION	V	ENGLOS	81.00	GICSA	4.64	ANTENNA DIAMETER (FT)	12.00	LOU	ANT HT	TIDE HT	D1	D2	PSI	RV	PHI	DR	M	F	DTM
FT	FT	FT	FT	FT	FT	FT	FT	FT	FT	FT	FT	FT	FT	FT	FT	FT	FT	FT	FT	FT	FT	FT	FT	FT	FT	FT	FT	FT	FT	FT	FT	FT	FT	FT	FT	FT	FT	FT	FT	FT	FT	FT	FT	FT	FT				
1600.00	4.00	6.65	37.47	0.21	0.98	26.34	306.51	0.52658E+00	-1.87	0.1168E+01																																							
1600.00	4.00	6.71	37.41	0.20	0.98	26.44	259.19	0.5237E+00	0.68	0.0984E+00																																							
1600.00	4.00	6.76	37.36	0.20	0.98	26.54	274.07	0.5207E+00	0.78	0.0104E+00																																							
1600.00	4.00	6.81	37.31	0.19	0.98	26.65	252.84	0.5175E+00	0.58	0.0965E+00																																							
1600.00	4.00	6.86	37.26	0.19	0.98	26.76	276.81	0.5141E+00	0.68	0.0105E+00																																							
1600.00	4.00	6.92	37.20	0.18	0.98	26.86	234.43	0.5104E+00	2.29	0.0896E+00																																							
1600.00	4.00	6.97	37.15	0.18	0.98	26.98	225.33	0.5066E+00	2.90	0.0859E+00																																							
1600.00	4.00	7.03	37.10	0.17	0.98	27.09	226.15	0.5026E+00	3.49	0.0716E+00																																							
1600.00	4.00	7.08	37.04	0.17	0.98	27.32	188.54	0.4983E+00	3.43	0.0685E+00																																							
1600.00	4.00	7.13	36.99	0.16	0.98	27.58	189.82	0.4943E+00	3.06	0.0548E+00																																							
1600.00	4.00	7.19	36.93	0.16	0.98	27.87	156.98	0.4893E+00	0.69	0.0452E+00																																							
1600.00	4.00	7.25	36.87	0.21	0.98	28.07	297.08	0.4843E+00	0.12	0.0352E+00																																							
1600.00	4.00	7.30	36.81	0.20	0.98	28.27	275.58	0.4793E+00	1.02	0.0252E+00																																							
1600.00	4.00	7.36	36.74	0.20	0.98	28.57	278.33	0.4743E+00	3.55	0.0152E+00																																							
1600.00	4.00	7.42	36.68	0.19	0.98	28.88	268.00	0.4693E+00	3.78	0.0095E+00																																							
1600.00	4.00	7.48	36.62	0.18	0.98	29.19	238.86	0.4643E+00	3.48	0.0079E+00																																							
1600.00	4.00	7.54	36.56	0.18	0.98	29.50	218.86	0.4593E+00	3.32	0.0072E+00																																							
1600.00	4.00	7.60	36.50	0.17	0.98	29.81	192.08	0.4543E+00	3.40	0.0063E+00																																							
1600.00	4.00	7.66	36.44	0.16	0.98	30.12	211.62	0.4493E+00	3.03	0.0051E+00																																							
1600.00	4.00	7.72	36.38	0.16	0.98	30.43	168.15	0.4443E+00	1.04	0.0042E+00																																							
1600.00	4.00	7.78	36.32	0.21	0.98	30.74	302.23	0.4393E+00	0.44	0.0038E+00																																							
1600.00	4.00	7.84	36.26	0.20	0.98	31.05	270.11	0.4343E+00	2.79	0.0036E+00																																							
1600.00	4.00	7.90	36.20	0.19	0.98	31.36	283.01	0.4293E+00	2.66	0.0028E+00																																							
1600.00	4.00	7.96	36.14	0.18	0.98	31.67	263.34	0.4243E+00	3.13	0.0026E+00																																							
1600.00	4.00	8.02	36.08	0.17	0.98	31.98	254.42	0.4193E+00	3.43	0.0019E+00																																							
1600.00	4.00	8.08	36.02	0.17	0.98	32.29	234.34	0.4143E+00	3.45	0.0017E+00																																							
1600.00	4.00	8.14	35.96	0.17	0.98	32.60	215.17	0.4093E+00	3.43	0.0014E+00																																							
1600.00	4.00	8.20	35.90	0.16	0.98	32.91	179.51	0.4043E+00	3.43	0.0011E+00																																							
1600.00	4.00	8.26	35.84	0.16	0.98	33.22	193.13	0.3993E+00	3.43	0.0008E+00																																							
1600.00	4.00	8.32	35.78	0.21	0.98	33.53	309.43	0.3943E+00	2.16	0.0005E+00																																							

[illegible]

Copyright © 1990 by the American Psychological Association  
0893-3200/90 \$3.00 + .00  
DOI: 10.1037/0893-3200.04.04.035

```

START OF DCEC HPRINT PROGRAM          DSNAM=E3893.LOS.FORT
REAL*4 MUT,MUTC,NUR,NURC,X,SITET(5),SITER(5),JST,KST,LAMPDA
REAL*4 M,LAM
C
C      INTEGER SITE
C
C      INTEGER*2 FOL,FOLLET(3)
C
C      COMPLEX Z,FV
C
C      DATA PCOLLET/'V','H','C'/
C
C      READING INPUT DATA
C
50 READ(5,5,END=20) HTGND,HTANT,HEGND,HRAnt,D,K,A,F,TH,TL,DTHL,HRMIN,
&DHF,POL,EPSLON,SIGMA,ANTD,SITET,SITER
FORMAT(8F10.0,/,5F10.0,4X,A1,5X,2F10.0,/,F10.0,1X,5A4,1X,5A4)
C
C      WRITING OUT INPUT DATA
C
WRITE(6,10) SITET,SITER,F,D,HTGND,HTANT,HEGND,HRAnt,K,A,TH,TL,
&DTHL,HRMIN,DHF,POL,EPSLON,SIGMA,ANTD
10 FORMAT(/, 'TRANSMITTER SITE ',2X,5A4,/,/, 'RECEIVER SITE ',2X,
&5A4,/,/, 'FREQUENCY (MHZ) ',F10.2,/,/, 'PATH LENGTH (MI) ',F8.2,/,/
&'TRANSMITTER SITE ELEVATION ABOVE MSL (FT) ',F8.2,/,/
&'TRANSMITTER ANTENNA HEIGHT ABOVE GROUND (FT) ',F8.2,/,/
&'RECEIVER SITE ELEVATION ABOVE MSL (FT) ',F10.2,/,/
&'RECEIVER ANTENNA HEIGHT ABOVE GROUND (FT) ',F8.2,/,/
&'EFFECTIVE EARTH RADIUS FACTOR ',F6.2,/,/, 'ACTUAL EARTH ',
&'DIAMETER (MI) ',F10.2,/,/, 'MAX HIGH TIDE ABOVE MSL (FT) ',F6.2,/,/
&'MAX LOW TIDE BELOW MSL (FT) ',F6.2,/,/, 'TIDE INCREMENT (FT) ',
&'F6.2,/,/, 'RECEIVER MINIMUM HEIGHT (FT) ',F10.2,/,/, 'RECEIVER ',
&'HEIGHT INCREMENT (FT) ',F6.2,/,/, 'POLARIZATION ',2X,A1,/,/, 'EP',
&'SLON ',F10.2,/,/, 'SIGMA ',F10.2,/,/, 'ANTENNA DIAMETER (FT) ',
&F10.2,/,/)
35 WRITE(6,35)
FORMAT(2X,'RCVR ANT HT',3X,'TIDE HT',8X,'D1',9X,'D2',9X,'PSI',8X,
&'R1',8X,'PHI',8X,'DR',10X,'Y',9X,'F',7X,'DTH')
45 WRITE(6,45)
FORMAT(7X,'FT',7X,'FT',10X,'S.MI',7X,'S.MI',8X,'DEG',19X,'DEG',
&87X,'DEG',6X,'VALUE',9X,'DB',7X,'NS'//)
C
C      CNST1 = 1.1547005
C      PI = 3.1415927
C      CONVERTS PATH LENGTH FROM STATUTE MILES TO FEET
C      D = D * 5280.
C      AE = EFFECTIVE EARTH RADIUS CONVERTED FROM STATUTE MILES TO FEET
C      AE = A * K * 5280.
25 HT = HTANT + HTGND - TH
HR = HEGND + HRAnt - TH
15 PSI = ATAN2((HT + HR),D)
SINPSI = SIN(PSI)
R1 = HT / SINPSI
R2 = HR / SINPSI
C
C      WRITE(6,1020) D,AE,HT,HR,PSI,SINPSI,R1,R2
1020 FORMAT('D = ',E12.4, 'AE = ',E12.4, 'HT = ',E12.4, 'HR = ',E12.4,
&'PSI = ',E12.4, 'SINPSI = ',E12.4, 'R1 = ',E12.4, 'R2 = ',E12.4)
C
C      WRITE(6,1000)
1000 FORMAT('AT 1ST SORT')
R = SORT((HR - HT)**2 + D**2)
DR = R1 + 12 - R
C
C      WRITE(6,1001)
1001 FORMAT('AT 2ND SORT')
SEE 26
STDEN = SORT(2. * AE * HT)
C
C      WRITE(6,1003)
1003 FORMAT('AT 3RD SORT')
SEE 26
SRDEN = SORT(2. * AE * HR)
C
C      WRITE(6,1006)
1006 FORMAT('AT 6TH SORT')
SEE 24
J = CNST1 * SORT(AE * (HT + HR) + (D/2. )**2)
C
C      SEE 25
FEE = ATCOS((2. * AE * (HR - HT) * D) / (2**3))
D2 = D / 2. + 2 * COS((FEE + PI) / 3.)
D1 = D - D2
LAMPDA = (2.E9 * 2.2808) / (F * 1.E6)
ST = D1 / STDEN
SR = D2 / SRDEN
C
C      WRITE(6,2002) R1,STDEN,R2,SRDEN,R
2002 FORMAT('R1 ',E12.4,2X,'STDEN ',E12.4,2X,'R2 ',E12.4,2X,'SRDEN ',

```

Copy available to DTIC does not  
 permit fully legible reproduction



[illegible]

UNCLASSIFIED

```

C      RVMAG = CABS(PV)                                000001
C      SEE P12M                                         000001
C      M = DST * RVMAG * ET * ER                      000001
C      GAMMA1 = 2. * PI * DRC / LAMBDA                 000001
C      WRITE(6,1031) DST,RV,RVMAG,ET,ER              000001
1031   FORMAT(' DST ',E12.4,2X,' RV ',E12.4,2X,' RVMAG ',E12.4,///,' ET ', 000001
      &E12.4,2X,' ER ',E12.4)                          000001
C                                                     000001
C      CALCULATING EPST,EPSR                          000001
C      CALL EPSTR(NUTC,EPST,ANTD,F)                   000001
C      CALL EPSTR(NUTC,EPSR,ANTD,F)                   000001
C      GAMMA = GAMMA1 - PI - EPST - EPSR              000001
C      COSGAM = COS(GAMMA)                            000001
C      WRITE(6,1007)                                   000001
1007   FORMAT(' AT 7TH S2RT')                          000001
C      SEE P12M                                         000001
C      ERDEFS = SQRT(1. + (M**2) + 2. * M * COSGAM)    000001
C      RFSDB = 20. * ALOG10(ERDEFS)                  000001
C      WRITE(6,1003) M,GAMMA,GAMMA1,EPST,EPSR,ERDEFS,RFSDB,COSGAM 000001
1003   FORMAT(' M = ',E12.4,' GAMMA = ',E12.4,' GAMMA1 = ',E12.4, 000001
      &' EPST = ',E12.4,' EPSR = ',E12.4,' ERDEFS = ',E12.4, 000001
      &' RFSDB = ',E12.4,' COSGAM = ',E12.4)            000001
C                                                     000001
C      D1 = D1 / 5280.                                000001
C      D2 = D2 / 5280.                                000001
C      PSIC = PSIC * 180. / PI                        000001
C      FEE = FEE * 180. / PI                          000001
C      HRMOD = HP + TH                                000001
C      WRITE(6,40) HRMOD,TH,D1,D2,PSIC,RVMAG,FEE,DRCDEG,M,RFSDB,DTM 000001
40     FORMAT(1X,8F11.2,E12.4,F11.2,E12.4)            000001
55     HR = HR - DHR                                    000001
C      HRMOD = HRMOD - DHR                             000001
C      IF(HRMOD.LE.HTGND) GO TO 30                    000001
C      IF(HRMOD.GE.HRMIN) GO TO 15                    000001
30     TH = TH - DTH                                    000001
C      IF(TH.GE.TL) GO TO 25                          000001
C      GO TO 50                                         000001
20     STOP                                             000002
C      END                                              000002
J      END OF DCEC UPRINT PROGRAM                      000002

```

LINES PRINTED= 202

Copy available to DTIC  
 permit fully legible reproduction

APPENDIX C

HYBRID SIMULATION OF THE DRAMA RADIO AND  
LINE-OF-SIGHT MULTIPATH CHANNEL

## INTRODUCTION

This appendix describes the modeling and simulation of (1) the line-of-sight (LOS) digital radio, AN/FRC-( ), which is being procured by the U.S. Army under the Digital Radio and Multiplexer Acquisition (DRAMA) program; and (2) a line-of-sight fading channel with individually controlled multiple paths. The simulation has been provided through a series of DCA R&D contracts with the Martin Marietta Corporation in Orlando, Florida. Using models and design data supplied by DCA, the DRAMA radio and LOS fading channel have been simulated on a hybrid computer system, as described in the following sections.

The hybrid computer simulation of the DRAMA radio, frequency selective fading line-of-sight channel, and performance indicating circuitry provides a programmable scale model which may be configured and changed to evaluate performance and design for any anticipated deployments. This model has been scaled down in time to permit simulation on the hybrid computer and special purpose hybrid delay line hardware. The current scale factor for the DRAMA radio simulation is 26,112 which results in simulated IF, data rate, and baseband frequencies of 2,681 Hz, 1,000 Hz, and 500 Hz, respectively.

## DRAMA RADIO

The hybrid computer model of the DRAMA radio includes all salient design and performance characteristics of this radio. These include Level I quadrature phase shift keyed (QPSK) performance at 13.065 Mb/s and Level II quadrature partial response (QPR) performance at 26.112 Mb/s. Other features are the switching of baseband filters for QPR and QPSK transmission, two and three level detection of the received baseband, and the signal processing needed to drive measurement, signal quality, and dual diversity switch circuits peripheral to the radio.

The DRAMA QPR/QPSK system simulation developed for this study is shown in Figure C-1. This figure shows the major simulation modules for data generation, input data signal processing, QPR/QPSK modulation, transmitter signal processing, dual LOS fading channels, dual diversity receivers, data regeneration, performance assessment, and diversity combining. Both Level I, QPSK, and Level II, QPR, transmission and receiving can be accomplished with this model. Design parameters for filters, data rates, phase lock loops (PPL), nonlinear devices, and signal quality monitors have been accounted for in the simulation model. Validation of the DRAMA system simulation has been based on actual bit error measurements taken from the DRAMA radio prototype. Figure C-2 provides plots of bit error probability versus signal-to-noise ratio\* for (1) DRAMA radio performance specification, (2) bit error measurement of DRAMA radio prototype, (3) DRAMA radio simulation and (4) theoretical performance for QPR modulation. Since the simulation on the hybrid computer should respond like the actual prototype, the simulated performance is degraded from theoretical. Note that both simulated and actual performance meet the performance level specified for the DRAMA radio.

\*Given in terms of energy per bit ( $E_b$ ) to noise power per Hz ( $N_0$ ).

The block diagram of Figure C-1 is briefly described here. A pseudorandom data stream (PRDS) representing digital traffic is generated in Module 1 of the simulation. In Module 2, the PRDS is scrambled using a self-synchronizing scrambler, split into cophasal and quadrature branches and differentially encoded. Up to this point the information is still in binary form. In Module 3, the cophasal and quadrature bit streams are presented to separate impulse modulators (actually pulse generators which generate very short pulses at the quadrature data rates). The outputs of the impulse modulators are presented to separate low pass filters which transform the binary cophasal and quadrature branches into three level baseband signals. Finally, in Module 3, the cophasal and quadrature bit streams are phase modulated onto a scaled IF (representing the actual 70 MHz IF of the AN/FRC-( ))( ) radio). Module 4 represents the RF stages of the AN/FRC-( ))( ) transmitter and includes a bandpass nonlinearity to represent the TWT RF amplifier amplitude together with post-amplification filtering.

Module 5 simulates the RF stages of the AN/FRC-( ))( ) receivers. Dual receivers are simulated to represent the dual diversity configuration of the radio and contain the IF filters (to provide frequency selectivity) as well as the Automatic Gain Control (AGC) function. In Module 6, the simulated IF QPR signal is demodulated by the modified Costas loop quadrature demodulator chosen by the AN/FRC-( ))( ) contractor. Module 6 also contains the carrier recovery and tracking circuitry and like Module 5, has redundant circuits to simulate a dual diversity radio configuration. The output of Module 6 is the analog version of the three-level partial response baseband which has an "eye pattern" representation. In Module 7, the diversity three-level basebands are regenerated by slicers, the bit timing is recovered, and now-digital three-level signals are decoded into several binary forms. Also, in Module 7 the diversity bit streams are descrambled for processing in the diversity switch.

In Module 8, in-service performance of the dual diversity bit streams is monitored. This module implements pseudo-error rate and AGC monitors for each of the diversity bit streams, and, based on a preprogrammable algorithm, develops a control voltage which is used to select the better diversity path in the AN/FRC-( ))( ) diversity combiner. In Module 9, the AN/FRC-( ))( ) dual diversity combiner is simulated. It is a selection combiner that uses an algorithm based on AGC and signal quality monitors.

#### LOS FADING CHANNEL

The fading channel model is implemented using a combination of hybrid computer technology and charge-coupled device (CCD) integrated circuits. The simulation consists of three elements: a delay line, a delay module, and a component fading module. A block diagram of the overall simulated channel is shown in Figure C-3. The delay line consists of a CCD integrated circuit with interconnection for up to 12 taps. The channel simulator actually has 2 delay lines, each having 12 taps. Delay line 1 is the in-phase tapped delay line, while the quadrature delay, line 2, contains an additional  $\pi/2$  phase shift at each tap. The complex multiplication required for setting the individual tap gains is shown functionally in Figure C-4. A wideband analog Gaussian noise

source provides noise to simulate fading conditions for each tap of the delay line. Multiplier pairs provide the multiplication of the incoming (delayed) path with noise for each of the 12 taps. The output of the 12 multiplier pairs is then summed by an analog summing amplifier network to provide the final channel output.

The simulator allows the user to select the number of active taps and change the tap gains, tap delay spacing, and signal-to-noise ratio. Also included is the capability to designate specific taps as Rayleigh fading or stationary, and to specify the correlation coefficient between the dual diversity fading signal envelopes from 0.10 to 0.95. The intertap spacing is selectable over two time scales: (1) 0.025 to 0.25 of a bit or (2) 0.25 to 2.5 of a bit. For a choice of QPR modulation with bit rate of 26.112 Mb/s, these two time scales provide the capability to simulate from approximately 1 to 100 nanoseconds. Referring to the block diagram in Figure C-4, a stationary tap is implemented from the Rayleigh fading tap by zeroing the quadrature coefficient and setting the in-phase coefficient to a constant value (determined from the relative mean power desired for that tap).

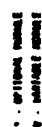


**Figure C-1. QPR and QPSK Dual Diversity Simulation**

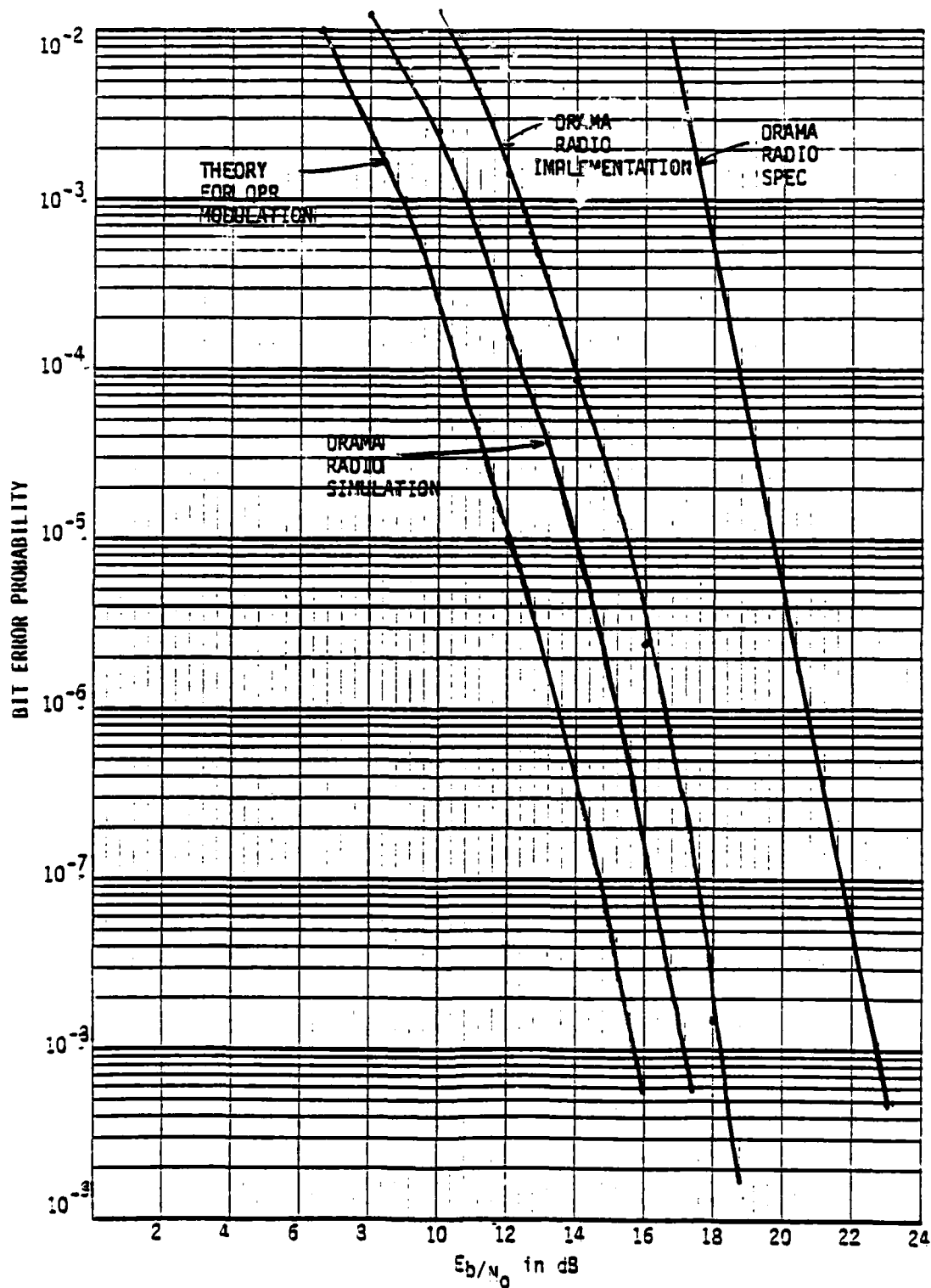
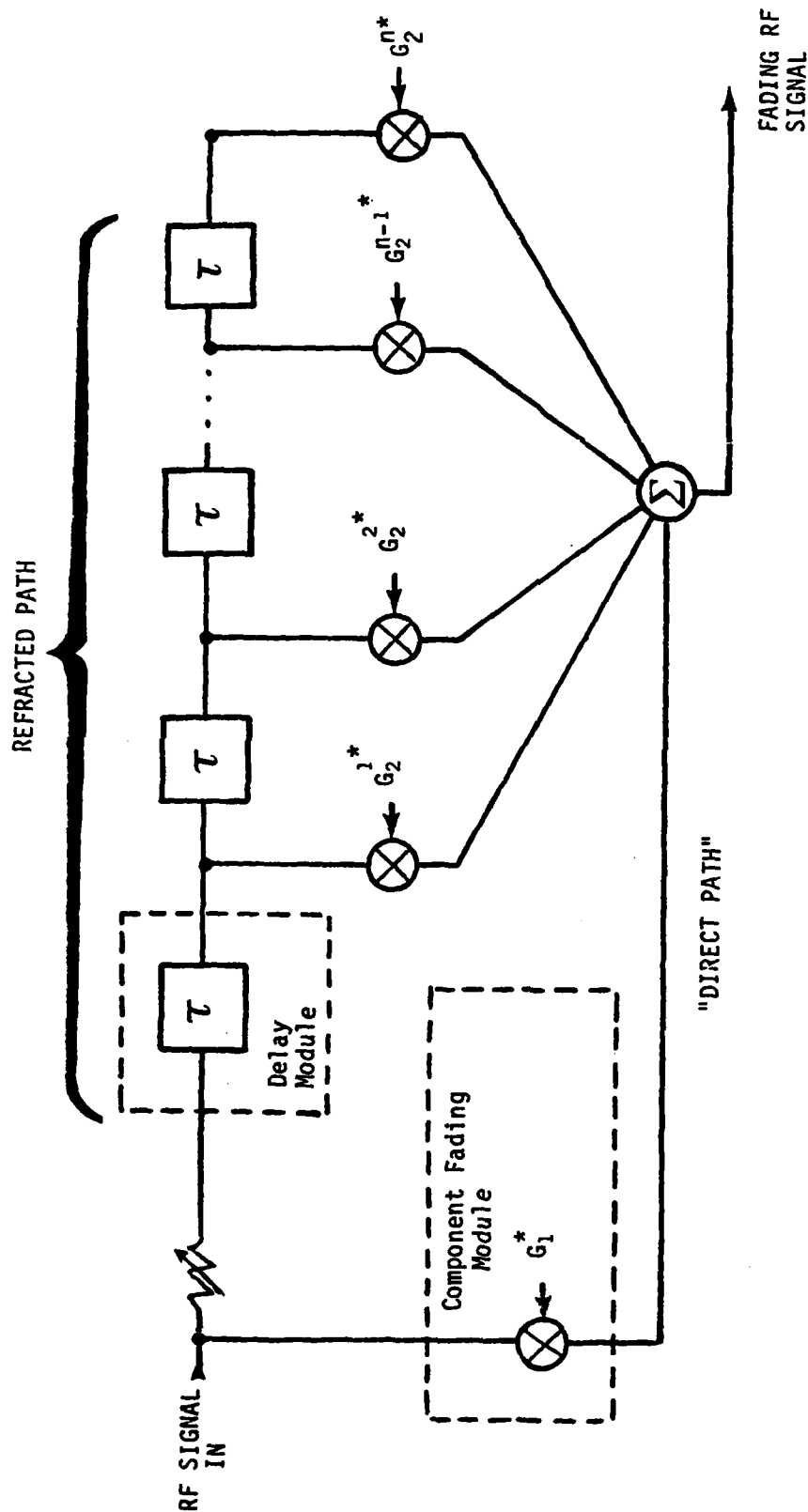


Figure C-2. Bit Error Probability Versus Signal-to-Noise Ratio for DRAMA Radio





NOTE:

$G_1^*$  - Complex Tap Weight for Direct Path

$G_2^{i*}$  - Complex Tap Weight for  $i$ th component of refracted path

$\alpha$  - Attenuator to vary direct/refracted path power ratio

Figure C-3. LOS Hybrid Computer Simulation (Single Diversity Channel)

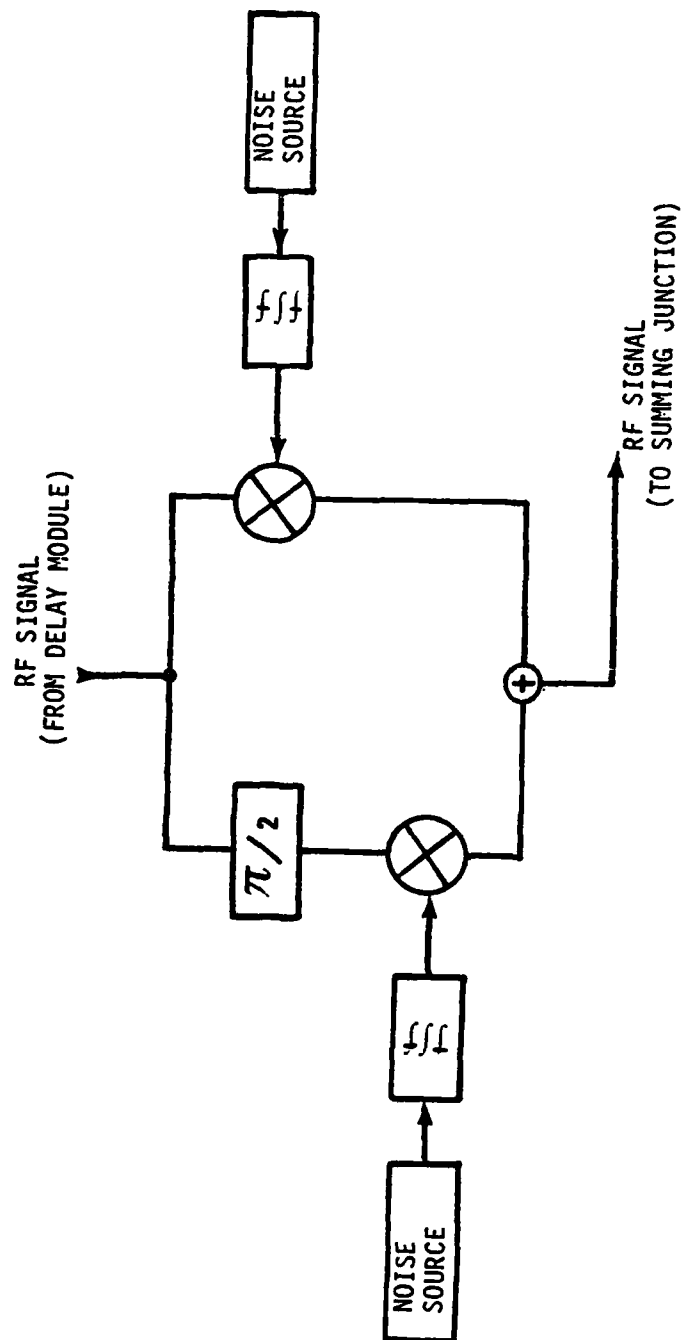


Figure C-4. Component Fading Module

APPENDIX D

SYNOPSIS OF SELECTIVE FADING TEST AND  
EVALUATION FOR DIGITAL LOS CHANNELS

## INTRODUCTION

Concern for the presence and effect of frequency selective fading on DCS digital links has prompted a number of DoD test and evaluation projects. This appendix briefly describes each of those projects in which DCA has some involvement.

Results of these T&E efforts will be used to (1) determine the need to make any necessary modifications to the DRAMA radio such as an improved diversity combiner or use of adaptive equalizer, and to (2) modify LOS channel models used by DCEC in providing guidance on DCS link design and availability objectives.

The milestone chart shown as Figure D-1 shows the phasing of these various T&E efforts.

### DEB I LINK TEST AND EVALUATION

This project consisted of a two month test conducted by the Institute of Telecommunications Sciences (ITS) under a DCA RDT&E contract. Data was collected within the Digital European Backbone Stage I (DEB I) on three LOS links (see Figure D-2) in the spring of 1980. The object of this set of measurements was to obtain statistics about presence and effect of distortion within the received IF spectrum of a 3-level partial response, line-of-sight microwave radio system.

Test instrumentation was installed at the Mt. Corna site which is the common site among the three DEB I links tested. Each link was monitored for evidence of selective fading but only the Mt. Venda-Mt. Corna link was found to exhibit any significant fading. The following signals were monitored, but recorded only if any activity was observed.

- (1) 70 MHz IF, both A and B receivers.
- (2) On-line receiver indicator.
- (3) Received signal level, both A and B receivers.
- (4) 3-Level errors.
- (5) Multiplex reframes.

Data was analyzed at the ITS Boulder Labs and results were published in DCEC Report No. 040022, March 1981. Salient conclusions were:

- (1) Large values of distortion (1 dB/MHz) were observed during multipath fading events.
- (2) Diversity reception looks very promising as an effective tool in counteracting these distortion effects.

(3) Multipath received-signal-level statistics can be used to predict the frequency and severity of this type of distortion on a line-of-sight path.

(4) The 3-level-partial-response modulation system used here was very robust in terms of its susceptibility to the severity of amplitude distortion observed on this path during the measurements.

#### WAWS LINK TEST AND EVALUATION

This RDT&E project consists of a two phase test and evaluation on the Washington Area Wideband System (WAWS) Blue Ridge Summit to Liberty Dam microwave path. Western Union is both the carrier providing the WAWS system as a lease to the U.S. Government and the contractor for this DCA RDT&E project. The object of this T&E effort is to obtain detailed statistics about the presence and effect of selective fading on wideband (30 MHz bandwidth, 90 Mbps data rate) digital LOS links. (The radio equipment tested was a Collins 8PSK digital radio operating in the 6 GHz band and employing space diversity.)

Phase I provided the following data on both receivers of the dual diversity system.

- a. Bit Error Rate (BER) measurements.
- b. IF Amplitude characteristics.
- c. Received Signal Level (RSL).

These data were monitored continuously with a granularity of 100 msec. As shown in Figure D-3, a computer was used to assemble this data from the BER test sets, the spectrum analyzer, RSL voltmeters, alarms and a clock (date/time) to form records. Under unfaded conditions, data records were not recorded to avoid storing useless data. Records were recorded only when fading activity was present as indicated by errors or changes in the spectrum or RSL. These data were then delivered on magnetic tape to DCEC for in-house analysis. Phase I data collection was conducted between October 1980 and February 1981, and in that time period about 73 days of valid data were observed. Most of the analysis has been completed with the following results:

- (1) Modest values of distortion (0.5 dB/MHz) were observed during fading events.
- (2) Deep fading events were rare: (1) the top receiver had a total of 16 seconds outage below RSL corresponding to  $BER = 10^{-7}$ ; (2) the bottom receiver had less than 1 second outage below RSL corresponding to  $BER = 10^{-7}$ .
- (3) The top receiver had 99.988802% error free blocks, and the bottom receiver had 99.999747% error free blocks, where the block length was approximately 100 msec of data.

Phase II data collection was completed in the summer of 1981 and provided the following data:

- a. Amplitude distortion.
- b. Group delay distortion.
- c. Received signal level.

As shown in Figure D-4, the same computer system was used to monitor the data, assemble the data into records and record these records on tape during periods of channel activity. Results from this second phase are necessary to characterize the channel for this 38 mile path. Such a channel characterization will in turn assist in the refinement of LOS channel models, taking into account the presence of frequency selective fading. Reduction and analysis of Phase II data is expected to be completed by March 1982.

#### DRAMA RADIO TEST AND EVALUATION

A three phased T&E program is currently planned for the DRAMA radio. These tests will characterize performance of the DRAMA radio in various multipath environment via simulation and, if possible, by actual link testing. A second objective is the characterization of multipath for typical DEB links. Once radio performance as a function of simulated or actual multipath conditions has been established, channel signatures for DEB and other DCS links can be used to predict outages due to multipath. Should outage predictions exceed DCA objectives, remedial action will consist of two possible actions:

- (1) Modification of DRAMA radio including consideration of improved diversity combining and adaptive equalization.
- (2) Modification of DCA link design criteria and link availability objectives.

Each of the three phases of testing is briefly described below:

##### (1) Multipath Simulation

USACEEIA at Ft. Huachuca has developed a three-ray multipath simulator in hardware to allow radio performance characterization. This simulator allows selection of the amplitude and delay for the multiple paths. Specifically, the attenuation of the direct path, ratio of amplitudes for the second and third paths, gross delay between direct and secondary paths, and phase of the sum of paths are selectable. A radio modem can be interfaced with the simulator (at 70 MHz IF), and for a particular combination of simulator settings, radio performance is characterized by measuring BER. To allow prediction of outage, a BER signature is developed which is a plot of constant BER (say for  $10^{-3}$  BER) as a function of delay and amplitude settings.

This simulator has been used to characterize performance of the AVANTEK DR 8-A modem, which operates at 12.6 Mb/s, uses QPR modulation, and has been used as a prototype in the DRAMA program. Results have been used in

conjunction with channel models, derived principally by Bell Labs, to predict outage as a function of link distance. A similar test and outage analysis is planned for the DRAMA radio modem in the July 1981 timeframe.

## (2) Pt. Mugu Link Tests

The Pacific Missile Test Center (PMTTC) at Point Mugu, California, is currently conducting multipath tests of a commercial digital radio over a 65 mile link between Pt. Mugu and San Nicolas Island. This long, over-the-water link is known to exhibit significant multipath, although the link is atypical of DCS links. Testing to date has involved a Collins 8 GHz, 44.7 Mb/s, 20 MHz bandwidth digital radio employing space diversity and adaptive equalization. Also a PN probe is being used to characterize the channel impulse response. Data collection is being provided by the Institute for Telecommunications Sciences (ITS), while data analysis is being done by PMTTC.

Testing of the DRAMA radio is planned for July-August 1981 over this same link at Pt. Mugu. Data collection and analysis is to be provided by ITS. The purpose of this test is to characterize radio performance over a link with known multipath conditions. Results will not be directly applicable to DEB links but through extrapolation and use of a channel model, these results will be of help in predicting performance on shorter links.

## (3) DEB Link Testing

Under USAF sponsorship and funding, channel characterization testing is being conducted for certain DEB links in the fall of 1981. Specifically, Langerkopf will be instrumented for data collection for up to three incoming LOS links. Tests are to be conducted by ITS using the PN probe and radio test instrumentation used previously at Pt. Mugu. Results of the PN probe tests will provide a multipath signature for these links tested. Using previous results of DRAMA radio testing at Pt. Mugu and at Ft. Huachuca with the multipath simulator, outage predictions will be possible for DEB.





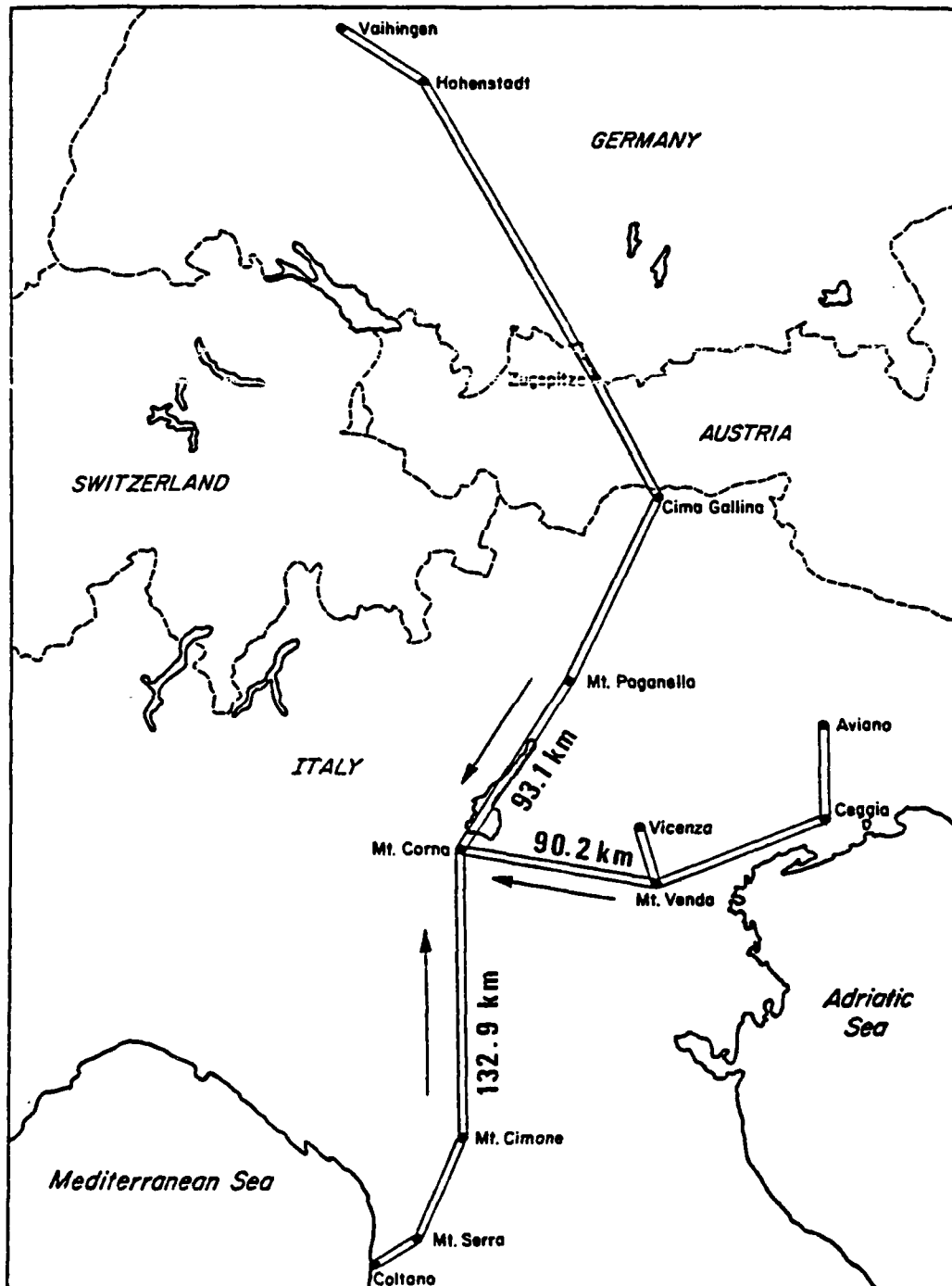


Figure D-2. Line-of-Sight Microwave Links Converging at Mt. Corna, Italy

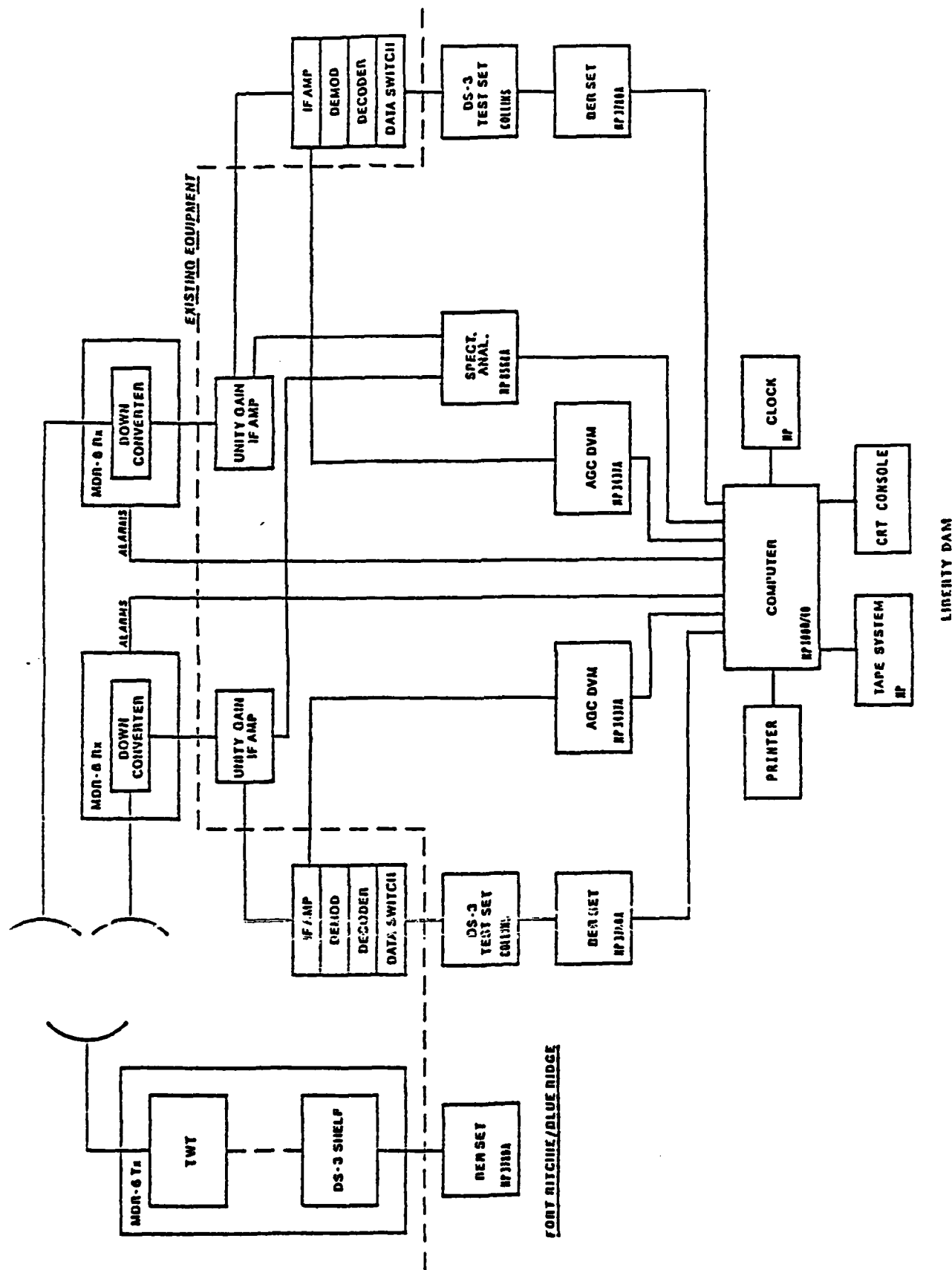


Figure D-3. Phase I - Test Configuration, Block Diagram

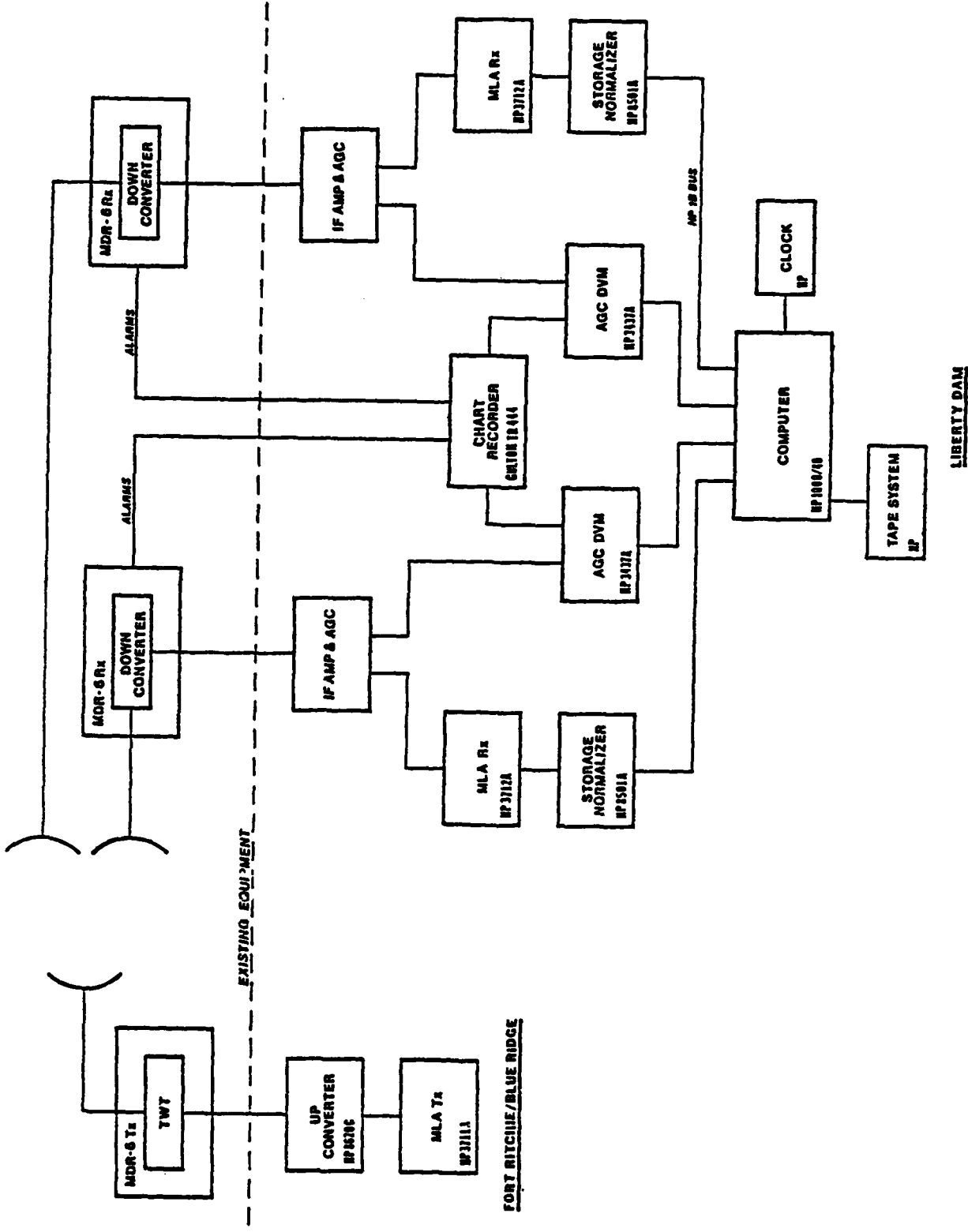


Figure D-4. Phase II - Test Configuration, Block Diagram

## DISTRIBUTION LIST

### STANDARD:

R100/R101 - 1	R400 -1
R120/R121/R140 - 1	R600 - 1
R141 - 9 (8 for stock)	R800 - 1
R110 - 1	NCS-TS - 1
R141B - 1 (Library)	101A - 1
R141A - 1 (for Archives)	312 - 1
R200 -1	970 -1

R141 - 12 (Unclassified/Unlimited Distribution)

DCA-EUR - 2 (Defense Communications Agency European Area  
ATTN: Technical Library  
APO New York 09131)

DCA-PAC - 3 (Commander  
Defense Communications Agency Pacific Area  
Wheeler AFB, HI 96854)

DCA SW PAC - 1 (Commander, DCA - Southwest Pacific Region  
APO San Francisco 96274)

DCA NW PAC - 1 (Commander, DCA - Northwest Pacific Region  
APO San Francisco 96328)

DCA KOREA - 1 (Chief, DCA - Korea Field Office  
APO San Francisco 96301)

DCA-Okinawa - 1 (Chief, DCA - Okinawa Field Office  
FPO Seattle 98773)

DCA-Guam - 1 (Chief, DCA - Guam Field Office  
Box 141 NAVCAMS WESTPAC  
FPO San Francisco 96630)

US NAV Shore EE PAC - 1 (U.S. Naval Shore Electronics Engineering  
Activity Pacific, Box 130, ATTN: Code 420  
Pearl Harbor, HI 96860)

1843 EE SQ - 1 (1843 EE Squadron, ATTN: EIEXM  
Hickam AFB, HI 96853)

DCA FO ITALY - 1 (DCA Field Office Italy, Box 166  
FPO New York 09524)

USDCFO - 1 (Unclassified/Unlimited Distribution)  
(Chief, USDCFO/US NATO  
APO New York 09667)

DISTRIBUTION LIST (cont'd)

SPECIAL:

PAC COMM DIV -1  
Hickam AFB, HI 96853

NAVTELCOMM 621A - 1  
Washington, DC 20390

NAV ELEC SYS COM 51032 - 1  
Washington, DC 20390

NAVCOMM AREA MASTER-MED - 1  
FPO NY 09524

NAVSHORE ELEC ENG ACT - 1  
FPO Seattle WA 97862

NAVSHORE ELEC ENG ACT - 1  
FPO San Francisco CA 96630

NAVCOMMSYSTECH SCHOOL - 1  
San Diego, CA 92133

NAVSHORE ELEC ENG ACT - PAC - 1  
Pearl Harbor, HI 96860

ECAC/CAA - 1  
Annapolis, MD 21402

RADC/DCCT - 1  
Griffiss AFB, NY 13441

CINCPAC/J6121 - 1  
FPO San Francisco 96558

